ELSEVIER

Contents lists available at ScienceDirect

Automatica

journal homepage: www.elsevier.com/locate/automatica



Switched control of an N-degree-of-freedom input delayed wearable robotic system[★]



Zhiyu Sheng a, Ziyue Sun b, Vahidreza Molazadeh a, Nitin Sharma a,b,*

- ^a Department of Mechanical Engineering and Materials Science, University of Pittsburgh School of Engineering, Pittsburgh, PA 15261, USA
- ^b Joint Department of Biomedical Engineering, North Carolina State University, Raleigh, NC 27606, USA

ARTICLE INFO

Article history: Received 26 December 2019 Received in revised form 16 August 2020 Accepted 19 November 2020 Available online xxxx

Keywords:
Wearable robotics
Input delay
Switched control
Multiple Lyapunov functional analysis

ABSTRACT

In this paper, a switched control method for a class of wearable robotic systems that prioritizes the use of human skeletal muscles in an assistive rigid powered exoskeleton is derived. A general N-degree-of-freedom (N-DOF) human-robot model is proposed to consider the challenges induced by the wearable system that include uncertainties and nonlinearities, unilateral actuation properties of the skeletal muscles, input delays, as well as a time varying actuator efficiency. Two control modes that alternatively switch and control a wearable robotic system are designed to overcome these challenges. A multiple Lyapunov functional analysis with state-dependent constraints on the switch criteria is performed to prove the stability. Simulations are performed to demonstrate the gain conditions, selected for each subsystem, that stabilize the overall system. Experiments on a human participant wearing a 4-DOF hybrid exoskeleton that combines functional electrical stimulation and a powered exoskeleton demonstrate the effectiveness of the switched control design.

© 2020 Elsevier Ltd. All rights reserved.

1. Introduction

Wearable robotic systems are increasingly being used for human augmentation in industrial and military applications (Cempini, De Rossi, Lenzi, Vitiello, & Carrozza, 2012; Choo & Park, 2017; De Looze, Bosch, Krause, Stadler, & O'Sullivan, 2016; Huo, Mohammed, Moreno, & Amirat, 2014; Walsh, 2018) and as assistive devices during rehabilitation (Cempini et al., 2012; Huo et al., 2014; In, Kang, Sin, & Cho, 2015; Jamwal, Xie, Hussain, & Parsons, 2012; Kim et al., 2012; Kubota et al., 2013; Pons, 2008, 2010). Recent papers on wearable robotic systems have used new control theory tools such as hybrid zero dynamics and energy shaping (Aroche, Meyer, Tu, Packard, & Arcak, 2019; Harib et al., 2018; Lv & Gregg, 2017). These control strategies for wearable robots primarily use actuation from electric motors. In contrast, the focus of our paper is a muscle first strategy control that enables a human user to maximize skeletal muscle use or harness muscle's inherent metabolic energy, via functional electrical stimulation (FES), and still use a rigid wearable robot.

The strategy is potentially beneficial from both rehabilitation and augmentation aspects. Firstly, compared to a case where a powered exoskeleton is used solely, a shared workload between externally stimulated muscles and a powered exoskeleton can reduce actuator and battery sizes, and thus make the overall system less bulkier. Secondly, the rigid exoskeleton uses electric motors to provide predictable torques. This attribute can be used to overcome relatively high nonlinearities and uncertainties that are in the musculoskeletal dynamics. These technical problems can also be relevant to another class of wearable robotic systems that comprise of soft robotic actuators such as, artificial muscles (Andrikopoulos, Nikolakopoulos, & Manesis, 2014; Caldwell, Medrano-Cerda, & Goodwin, 1995; Chou & Hannaford, 1996; Daerden & Lefeber, 2002; Reynolds, Repperger, Phillips, & Bandry, 2003; Tondu & Lopez, 2000). Unmodeled phenomenon and hysteresis effects (Vo-Minh, Tjahjowidodo, Ramon, & Van Brussel, 2010) can add nonlinear effects and uncertainties during soft actuator control (Mirvakili & Hunter, 2018). The control of these soft actuators may be improved by using them in conjunction with a light weight rigid robot.

We propose a general class of hybrid wearable robotic system comprising of a muscle/soft actuator and a rigid robot, where the latter can be substituted in an event of a degraded control performance or reduced actuator efficiency that otherwise may impair control effectiveness. For example, the reduced actuator efficiency is usually observed during FES of skeletal muscles where a rapid onset of the muscle fatigue reduces a muscle's

This research is supported by NSF, USA award number: 1646009. The material in this paper was presented at the 2018 American Control Conference, June 27–29, 2018, Milwaukee, WI, USA. This paper was recommended for publication in revised form by Associate Editor Ciro Natale under the direction of Editor Thomas Parisini.

^{*} Correspondence to: 1840 Entrepreneur Drive 4212C Engineering Building III Raleigh, NC, 27695, USA.

E-mail addresses: zhs41@pitt.edu (Z. Sheng), zsun32@ncsu.edu (Z. Sun), vam50@pitt.edu (V. Molazadeh), nsharm23@ncsu.edu (N. Sharma).

Z. Sheng, Z. Sun, V. Molazadeh et al. Automatica 125 (2021) 109455

force output. As a result of this combination, this general class of hybrid wearable robotic system possesses distinct dynamic characteristics of skeletal muscles (or soft actuators) and a rigid powered exoskeleton. These characteristics include unilateral actuators that produce force only in one direction. Due to this unilateral force generation, these soft actuators have to be implemented as an agonist-antagonist pair to produce bidirectional torques at each robotic joint. Further, fluid-based actuation or slow activation of human muscles may introduce electromechanical delays (EMD) (Sharma, Gregory and Dixon, 2011), a form of input delay, in the wearable system. The control of this class of wearable robots is further complicated by the presence of nonlinearities and uncertainties in the human-robot model and a need to maintain performance in the event of loss of control effectiveness. In view of these challenges, this class of wearable robot system may necessitate use of switched control.

A switched control method for an N-degree-of-freedom (N-DOF) general class of wearable robotic systems is proposed in this paper. The resulting hybrid system is driven by two control modes: I and II, and a switch signal that indicates the control mode. Mode I aims at addressing the input delay problem and applies a PD-based controller for a combined use of skeletal muscle/soft actuator and electric motors. General gain conditions to adjust the muscle-motor contributions are derived. Mode II utilizes electric motors with a smooth variable structure controller (VSC) (Zinober, 1994) to actuate all of the N limb joints when the actuator efficiency approaches a designed threshold.

The two main contributions of this paper are considering distinct input delays in the wearable robotic system and new state-dependent constraint conditions in a multiple Lyapunov functional approach for switched systems. Here we discuss the two contributions. Firstly, a proportional derivative (PD) based control strategy that compensate for EMDs is developed in a general N-DOF system. Input delay problems of nonlinear control systems have recently been explored in Alibeji, Kirsch, Dicianno, and Sharma (2017), Bekiaris-Liberis and Krstic (2012), Krstic (2009), Lei and Khalil (2015, 2016), Nihtilä (1989), Polyakov, Efimov, Perruquetti, and Richard (2013), Sharma, Bhasin, Wang and Dixon (2011) and Sharma, Gregory et al. (2011). Compared to those, in this paper, a particular challenge is introduced by distinct EMDs, $\tau_i^{(j)}$, in the muscles or soft actuators of an agonist-antagonist pair (j = 1, 2) at different joints (i = 1, 2, ..., N). By considering this challenge, the result of this paper generalizes the analysis in Sharma, Bhasin et al. (2011) from a uniform input delay, τ , to $\tau_i^{(j)}$ and applies the control design in the model of a general wearable robotic system. Accordingly, delay compensation terms are specifically designed for each muscle/actuator group and Lyapunov-Krasovskii (L-K) functionals are chosen to prove the stability of the N-DOF system under the developed controller.

Secondly, the stability of the switched N-DOF wearable robotic system is analyzed via a multiple Lyapunov functional (MLF) (Branicky, 1998; DeCarlo, Branicky, Pettersson, & Lennartson, 2000; Goebel, Sanfelice, & Teel, 2009; Liberzon & Morse, 1999) approach, provided that each subsystem in the switch family is proven to attain a semi-globally uniformly ultimately bounded (sGUUB) stability. In Kirsch, Alibeji, Dicianno, and Sharma (2016), a similar fatigue-motivated switched strategy was proposed for a single DOF hybrid neuroprosthesis. A common second order sliding mode controller was designed based on a feedback linearized virtual input that was used for both muscles and motors. The stability of the switched system was then analyzed by a common Lyapunov functional (CLF) (Liberzon & Morse, 1999). Downey, Cheng, Bellman, and Dixon (2017) also used a CLF to prove the stability of a 1-DOF lower-limb neuroprosthetic system. Asynchronous stimulation of different muscle groups was modeled as a switched system. However, in our current paper, due to the existence of the delay compensation terms and the corresponding L-K functional, it is difficult to find an explicit CLF that guarantees the arbitrary (fast) switch. Instead, different Lyapunov functionals have to be considered to facilitate different control modes. As a result, when the subsystems are combined, discontinuity of the Lyapunov functional occurs at each switch. In this situation, typically, a dwell time approach is employed in an MLF analysis to guarantee the stability. However, due to the dwell time, the unnecessary waiting period between switches, in general, might be undesirable for human augmentation or rehabilitation. Therefore, in the MLF analysis of this paper, we explicitly derive additional constraints in the switch criteria to not only guarantee the overall stability, but also enable a desired switch immediately once those constraints are satisfied.

A preliminary conference paper on a 5-DOF lower-limb human-robot model with a uniform input delay at knee joints was presented in Sheng, Molazadeh, and Sharma (2018). In the current paper, the theoretical results have been extended to a general N-DOF system with different input delays of each soft actuator at each joint. The control mode II has also been modified to use the VSC controller with a continuous input. A new Lemma 1 has been introduced to perform the switch criteria that fully depend on the measurable states and estimated model parameters. This guarantees the feasibility of experiment implementation. New simulations that show the use of gain conditions and experimental results with a human participant that validate the controller have also been added.

Notation: For simplicity, in this paper, $(v_i)_N$ represents a vector $v=(v_1,v_2,\ldots,v_N)^T\in\mathbb{R}^N$ and $\left(a_{ij}\right)_{M\times N}\in\mathbb{R}^{M\times N}$ represents a matrix array. $v_\tau=v(t-\tau)=(v_i(t-\tau_i))_N=\left(v_{i,\tau_i}\right)_N\in\mathbb{R}^N$ denotes the vector v after each element, as a time dependent function, being delayed by $\tau_i, (i=1,2,\ldots,N)$. Time dependent functions can be simplified as $v(t)=v\in\mathbb{R}^N$ when there is no time delay.

Remark. The work here is motivated from FES-based control of skeletal muscles in a hybrid exoskeleton. However, we interchangeably denote muscles as soft actuators. This is a slight abuse of the terminology used by the soft actuator community. The terminology is interchangeably used to extend the proposed switched framework to a general class of wearable exoskeleton that combine FES control of skeletal muscles or soft actuators with a powered exoskeleton.

2. Modeling

A generalized N-DOF model for a wearable robotic system is expressed by the Euler-Lagrange (E-L) equations:

$$D(q)\ddot{q} + C(q, \dot{q})\dot{q} + G(q) + M_{ev}(q, \dot{q}) + W$$

$$= T_s^{(1)} - T_s^{(2)} + T_m,$$
(1)

where $q(t)=(q_i(t))_N\in\mathbb{R}^N$ are time dependent limb joint angles. $D(q)\in\mathbb{R}^{N\times N},\ C(q,\dot{q})\in\mathbb{R}^{N\times N},\$ and $G(q)\in\mathbb{R}^N$ are a generalized inertia matrix, a Coriolis–centripetal matrix and a gravity vector, respectively. $M_{ev}(q,\dot{q})\in\mathbb{R}^N$ expresses passive moments due to the elastic-viscous effect at each limb joint. $W\in\mathbb{R}^N$ represents a disturbance term. $T_s^{(j)}(t)=\left(T_{s,i}^{(j)}(t)\right)_N\in\mathbb{R}^N$ is

a vector that represents torques contributed by each actuator: j, where j=1,2, of an agonist-antagonist soft actuator pair at a joint: i, where $i=1,2,\ldots,N$. $T_m(t)=\left(T_{m,i}(t)\right)_N\in\mathbb{R}^N$ is a vector that represents torques exerted by electric motors of a rigid exoskeleton at a joint: i. The torque exerted by the electric motor at a joint i is modeled according to a linear relationship,

$$T_{m,i} = K_{m,i} u_{m,i}, \tag{2}$$

where $K_{m,i} \in \mathbb{R}_{>0}$ is a motor constant and $u_{m,i}(t) \in \mathbb{R}$ is an input to the electric motor. The N-DOF model is developed under the following assumptions:

(A1) Modeling of $T_s^{(j)}$ and distinct input delays. The torque produced by a soft actuator j at a joint i is modeled as

$$T_{s,i}^{(j)} = \hat{\mu}_i^{(j)} \eta_i^{(j)} u_{a,i,\tau}^{(j)}, \tag{3}$$

where $\eta_i^{(j)}(q,\dot{q}) \in \mathbb{R}_{>0}$ is a lumped bounded unknown nonlinear function that maps a positive input delayed control signal $u_{a,i,\tau_i^{(j)}}^{(j)} = u_{a,i}^{(j)}(t-\tau_i^{(j)}) \in \mathbb{R}_{>0}$ to $T_{s,i}^{(j)}$. $\tau_i^{(j)} \in \mathbb{R}_{>0}$ is the EMD

associated with the actuator j at joint i. $\tau_i^{(j)}$ values are assumed as known constants but can have distinct values for different i and j.

(A2) Time-variant actuator efficiency. Motivated from the phenomenon of the human muscle fatigue (Sharma, Kirsch, Alibeji, & Dixon, 2017), we introduce a time-variant term, $\hat{\mu}_i^{(j)}(t) \in [\varsigma_i^{(j)}, 1]$, as the estimate of the actuator efficiency. $\varsigma_i^{(j)} \in \mathbb{R}$ is the lower bound of $\hat{\mu}_i^{(j)}$ and $\hat{\mu}_i^{(j)}$ is assumed to follow a known continuous governing equation that models the fatigue and recovery process, as

$$\dot{\hat{\mu}}_{i}^{(j)} = \Gamma_{i}^{(j)}(\hat{\mu}_{i}^{(j)}, u_{a,i,\tau_{i}^{(j)}}^{(j)}). \tag{4}$$

(A3) The disturbance, W(t), and the unknown functions: $M_{ev}(q, \dot{q})$ and $\eta_i^{(j)}$ are bounded.

3. Control design

3.1. Two control modes in the switched N-DOF human-robot system

Two control modes are integrated to control the N-DOF system in (1). In mode I, torque contributions from soft actuators and assistive electric motors can share work load. The input to the soft actuators in (3) is designed as

$$u_{a,i}^{(j)} = \frac{1+\xi}{2} K_{a,i}^{(j)} u_{s,i}^{(j)}, \tag{5}$$

where $u_{s,i}^{(j)}(t) \in \mathbb{R}_{>0}$ is the subsequently designed proportional derivative (PD) feedback controller with a compensation term for different EMDs. $K_{a,i}^{(j)} \in \mathbb{R}$ is an additional gain to modulate $u_{s,i}^{(j)}$ of individual actuators. $\xi(t) \in \{-1,1\}$ is a switch signal. $\xi=1$ indicates mode I and $\xi=-1$ indicates mode II. After substituting (5) into (3), the torque contribution from the soft actuator is expressed as

$$T_{s,i}^{(j)} = \frac{1 + \xi_{\tau_i^{(j)}}}{2} \hat{\mu}_i^{(j)} \eta_i^{(j)} K_{a,i}^{(j)} u_{s,i,\tau_i^{(j)}}^{(j)}.$$
 (6)

By adding the switch signal to (2), electric motor torque contributions are expressed as

$$T_{m_l,i} = \frac{1+\xi}{2} K_{m,i} u_{m_l,i},\tag{7}$$

where $u_{m_I,i} \in \mathbb{R}$ denotes the control input to the electric motor under mode I.

When mode II ($\xi = -1$) is activated, all the joints are driven by torque contributed from electric motors as

$$T_{m_{II},i} = \frac{1-\xi}{2} K_{m,i} u_{m_{II},i}, \tag{8}$$

where $u_{m_{I\!I},i} \in \mathbb{R}$ is the control input to the electric motor under mode II.

By combining mode I and mode II and using (1), (6), (7) and (8), the N-DOF system under a switched control of the defined

actuators can be expressed as

$$D(q)\ddot{q} + C(q, \dot{q})\dot{q} + G(q) + M_{ev}(q, \dot{q}) + W$$

$$= \left(\frac{1 + \xi_{\tau_{i}^{(1)}}}{2}\hat{\mu}_{i}^{(1)}\eta_{i}^{(1)}K_{a,i}^{(1)}u_{s,i,\tau_{i}^{(1)}}^{(1)}\right)_{N}$$

$$- \left(\frac{1 + \xi_{\tau_{i}^{(2)}}}{2}\hat{\mu}_{i}^{(2)}\eta_{i}^{(2)}K_{a,i}^{(2)}u_{s,i,\tau_{i}^{(2)}}^{(2)}\right)_{N}$$

$$+ \left(\frac{1 + \xi}{2}K_{m,i}u_{m_{I},i}\right)_{N} + \left(\frac{1 - \xi}{2}K_{m,i}u_{m_{II},i}\right)_{N},$$
(9)

which consists of two subsystems indexed by the switch signal, $\xi(t)$. For simplicity of the subsequent derivations, we denote $\hat{\mu}^{(j)} = \left(\hat{\mu}_i^{(j)}\right)_N \in \mathbb{R}^N$, $\eta^{(j)} = \left(\eta_i^{(j)}\right)_N \in \mathbb{R}^N$, $u_s^{(j)} = \left(u_{s,i}^{(j)}\right)_N \in \mathbb{R}^N$, $u_{m_1} = \left(u_{m_1,i}\right)_N \in \mathbb{R}^N$.

3.2. The state vector of trajectory tracking and delay compensation

The control objective is to make the switched system, (9), track a desired trajectory, $q_d(t) = \left(q_{d_i}(t)\right)_N \in \mathbb{R}^N$ under the following assumption:

(A4) The desired trajectories and their time derivatives are known and bounded.

The tracking error $e(t) = (e_i(t))_N \in \mathbb{R}^N$ is defined as

$$e_i = q_{d,i} - q_i. \tag{10}$$

To facilitate the control development and the stability analysis, the auxiliary signal $r(t) \in \mathbb{R}^N$ is

$$r = \dot{e} + \alpha e - \frac{\xi + 1}{2} \beta e_c, \tag{11}$$

where

$$e_c(t) = \left(e_{c,i}^{(1)}\right)_N - \left(e_{c,i}^{(2)}\right)_N \tag{12}$$

is a delay compensation vector defined as

$$e_{c,i}^{(j)} = \int_{t-\tau_c^{(j)}}^t u_{s,i}^{(j)}(\theta) d\theta.$$
 (13)

 $\alpha, \beta \in \mathbb{R}_{>0}$ are constant gains. The error signal, r, that contains velocity error information has the piecewise continuous property. To facilitate the input delays, the delay compensation term in (11) is only used in mode I; i.e., when $\xi = 1$. (11) and (13) consider that the values of the input delays are different for each unilateral soft actuator. Using the tracking errors e, r, the switch signal, ξ , and the efficiency state, $\hat{\mu}^{(j)}$, a state vector $y \in \mathcal{U}$ is defined as

$$y = \left[e^{T}, r^{T}, \hat{\mu}^{(1)^{T}}, \hat{\mu}^{(2)^{T}}, \xi \right]^{T}, \tag{14}$$

where $\mathcal{U}=\mathbb{R}^{2N}\times[\varsigma_1^{(1)},1]\times[\varsigma_2^{(1)},1]\times\cdots\times[\varsigma_N^{(1)},1]\times[\varsigma_1^{(2)},1]\times$ $[\varsigma_2^{(2)},1]\times\cdots\times[\varsigma_N^{(2)},1]\times[-1,1].$ To achieve the control objective and to also maintain the efficiency of the muscle/soft actuator, the following sections describe the design of the control inputs: $u_s^{(j)},u_{m_l},u_{m_{ll}}$, and the switch criteria that is dependent on the state vector, y.

3.3. Feedback control law and closed loop error dynamics

3.3.1. *Mode I:* $\xi = 1$

The feedback control law for $u_s^{(j)}$ and u_{m_l} that determines mode I is designed as

$$\begin{pmatrix} u_s^{(1)} \\ u_s^{(2)} \\ u_{m_l} \end{pmatrix} = K_u \begin{pmatrix} Q_1^{(1)} Q_2 Q_3 \\ Q_1^{(2)} Q_2 Q_3 \\ Q_4 \end{pmatrix} r,$$
(15)

where $Q_1^{(1)}$, $Q_1^{(2)}$, Q_2 , Q_3 , $Q_4 \in \mathbb{R}^{N \times N}$ are

$$Q_{1}^{(1)} = \operatorname{diag}\left(\frac{1 + \operatorname{sgn}(r_{1})}{2}, \frac{1 + \operatorname{sgn}(r_{2})}{2}, \dots, \frac{1 + \operatorname{sgn}(r_{N})}{2}\right),$$

$$Q_{1}^{(2)} = \operatorname{diag}\left(\frac{1 - \operatorname{sgn}(r_{1})}{2}, \frac{1 - \operatorname{sgn}(r_{2})}{2}, \dots, \frac{1 - \operatorname{sgn}(r_{N})}{2}\right),$$

$$Q_{2} = \operatorname{diag}\left(\rho_{s,1}, \rho_{s,2}, \dots, \rho_{s,N}\right),$$

$$Q_{3} = \operatorname{diag}\left(\operatorname{sgn}(r_{1}), \operatorname{sgn}(r_{2}), \dots, \operatorname{sgn}(r_{N})\right),$$

$$(16)$$

 $Q_4 = \left(\begin{array}{c} \rho_{m,ij} \end{array} \right)_{N \times N}.$

 $K_u \in \mathbb{R}_{>0}$, $\rho_{s,i} \in \mathbb{R}_{>0}$, are constant control gains. $\rho_{m,ij} \in \mathbb{R}$, represents the variable control gains of the electric motors. The sgn (\cdot) function is used in view of the unilateral property of the soft actuators and to facilitate control of an agonist–antagonist pair. When, $\xi = 1$, by differentiating both sides of (11), then multiplying by D(q), using (9) and (10), and substituting (15), the closed loop error dynamics of the subsystem $(\xi = 1)$ is obtained as

$$D(q)\dot{r} = -\frac{1}{2}\dot{D}(q)r - e + \tilde{\Phi} + \Phi_d + W$$

$$-\hat{D}(q)\beta K_u Q_2 r - K_M K_u Q_4 r$$

$$-\tilde{D}(q)\beta K_u Q_2 r$$

$$+\beta H^{(1)}K_u Q_{1,\tau(1)}^{(1)} Q_2 Q_{3,\tau(1)} r_{\tau(1)}$$

$$-\beta H^{(2)}K_u Q_{1,\tau(2)}^{(2)} Q_2 Q_{3,\tau(2)} r_{\tau(2)},$$
(17)

where $Q_{1\tau(1)}^{(1)}$, $Q_{1,\tau(2)}^{(2)}$, $Q_{3,\tau(1)}^{(1)}$ and $Q_{3,\tau(2)}^{(2)}$ are defined by delaying each $r_i(t)$ signal in (16) by $\tau_i^{(1)}$ or $\tau_i^{(2)}$. $H^{(j)} \in \mathbb{R}^{N \times N}$ is

$$H^{(j)} = D(q) - \frac{1}{\beta} \operatorname{diag} \left(\hat{\mu}_1^{(j)} \eta_1^{(j)}, \hat{\mu}_2^{(j)} \eta_2^{(j)}, \dots, \hat{\mu}_N^{(j)} \eta_N^{(j)} \right) K_A^{(j)}.$$

 K_M and $K_{a,i}^{(j)}$ are diagonal matrices of the motor constant, $K_{m,i}$, and gains, $K_{a,i}^{(j)}$, defined in (2) and (5), respectively, and $\hat{D} \in \mathbb{R}^{N \times N}$ is an estimate of D. Therefore, the estimation error $\tilde{D} \in \mathbb{R}^{N \times N}$ is $\tilde{D} = D - \hat{D}$. In (17), $\tilde{\Phi} \in \mathbb{R}^N$ is $\tilde{\Phi} = \Phi - \Phi_d$, where $\Phi(t)$, $\Phi_d(t) \in \mathbb{R}^N$ are defined as

$$\Phi = \frac{1}{2}\dot{D}r + e + D(\ddot{q}_d + \alpha\dot{e}) + C\dot{q} + G + M_{ev},
\Phi_d = D(q_d)\ddot{q}_d + C(q_d, \dot{q}_d)\dot{q}_d + G(q_d) + M_{ev}(q_d, \dot{q}_d).$$
(18)

According to Sadegh and Horowitz (1990) and the assumption (A3) and (A4), it can be proven that

$$\|\tilde{\Phi} + \Phi_d + W\| \le \delta \Phi(\|z\|) \|z\| + \Psi,$$
 (19)

where $z \in \mathbb{R}^{4N}$ is $z = (e^T, r^T, e_c^{(1)^T}, e_c^{(2)^T})^T$. $\delta \Phi(\cdot)$ is a positive globally invertible non-decreasing function. $\Psi \in \mathbb{R}_{>0}$ is a constant.

3.3.2. *Mode II*: $\xi = -1$

In mode II, the robust VSC controller, $u_{m_{II}}(t)$, is designed as

$$u_{m_{II}} = K_{M}^{-1} \left(\frac{r}{\|r\| + r_{c}} \left(\delta \Phi'(\|y_{er}\|) \|y_{er}\| + \Psi' \right) + K_{v} r \right), \tag{20}$$

where $y_{er}=(e^T,r^T)^T$. $K_v\in\mathbb{R}_{>0}$ is a constant control gain. $r_c\in\mathbb{R}_{>0}$ is a small constant. $\delta\Phi'(\cdot)$, which is a positive globally invertible non-decreasing function, and $\Psi'\in\mathbb{R}_{>0}$ are guessing functions to bound $\|\tilde{\Phi}+\Phi_d+W-\tilde{B}\|$. They satisfy

$$\left\|\tilde{\Phi} + \Phi_d + W - \tilde{B}\right\| \le \delta \Phi'(\|y_{er}\|) \|y_{er}\| + \Psi',$$

where $\tilde{B} \in \mathbb{R}^N$ is the remaining bounded actuation from mode I due to EMD after the most recent switch and will certainly

disappear in a short time period, $\max_i \{\tau_i\}$. By using the same derivation as in the case when $\xi = 1$ but substituting (20) for the control input, the closed loop error dynamics corresponding to the subsystem ($\xi = -1$) of (9) is derived as,

$$D(q)\dot{r} = -\frac{1}{2}\dot{D}(q)r - e + \tilde{\Phi} + \Phi_d + W - \tilde{B}$$

$$-\frac{r}{\|r\| + r_c} \left(\delta\Phi'(\|y_{er}\|) \|y_{er}\| + \Psi'\right) - K_v r.$$
(21)

3.4. Switch criteria

According to (3), the torque generated under a certain input can vary with the actuator efficiency. To obtain a consistent joint torque, these actuators can be switched with electric motors when the efficiency is low and re-activated upon recovery. Therefore, a switch logic is designed to determine the choice between the subsystems, $\xi = 1$ or $\xi = -1$. This behavior is modeled as

$$\xi^{+} = -\xi^{-} \quad (e^{-T}, r^{-T}, \mu^{-T}, \xi^{-})^{T} \in \mathcal{D} \quad , \tag{22}$$

where $(\cdot)^-$ and $(\cdot)^+$ denote the value just before and after the switch. The set $\mathcal D$ consists the union of three sets and forms the switch criteria, as

$$\mathcal{D} = \left\{ y \in \mathcal{U} : \xi = 1, \exists j \in \{1, 2\}, i \in \{1, 2, \dots, N\} \right\}$$

$$\text{s.t.} \hat{\mu}_{i}^{(j)} \leq \underline{\mu} \right\} \cup \mathcal{D}_{er\xi} \cup \left\{ y \in \mathcal{U} : (e^{T}, r^{T}, \xi) \in \mathcal{D}'_{er\xi_{l}}, \right.$$

$$\forall j \in \{1, 2\}, i \in \{1, 2, \dots, N\} \text{ s.t.} \hat{\mu}_{i}^{(j)} \geq \overline{\mu} \right\}. \tag{23}$$

 $\underline{\mu},\overline{\mu}\in[\max_{i,j}\left\{\varsigma_i^{(j)}\right\},1],\ \underline{\mu}<\overline{\mu},$ are constants that describe the lower and upper thresholds of the efficiency states to enable the switch. After one of the efficiency states drops below the designed threshold, $\underline{\mu}$, system will utilize the control mode II, (subsystem $\xi=-1$) instead of the control mode I, (subsystem $\xi=1$), until all of the those states recover to the designed values, $\overline{\mu}$. $\mathcal{D}_{er\xi}$, and $\mathcal{D}_{er\xi}'$ are additional state dependent conditions to be designed so that overall stability of (9) for tracking a desired trajectory can be ensured in the presence of switches.

4. Stability of the subsystems

The following properties and definitions will be used during the stability analysis.

$$\sigma_1 \|r\|^2 \le r^T Dr \le \sigma_2 \|r\|^2$$
. (24)

$$\lambda_1 \|y_{er}\|^2 \le \frac{1}{2} e^T e + \frac{1}{2} r^T Dr \le \lambda_2 \|y_{er}\|^2.$$
 (25)

 $r^T H^{(j)} Q_{1,\tau^{(j)}}^{(j)} Q_2 Q_{3,\tau^{(j)}}^{(j)} r_{\tau^{(j)}}$

$$\leq \sigma_3^{(j)} \bar{\rho}_s \| r \| \| Q_{1\tau(j)}^{(j)} r_{\tau(j)} \|, |\sigma_3^{(j)}| \leq \bar{\sigma}_3^{(j)}. \tag{26}$$

$$r^{\mathsf{T}}\tilde{\mathsf{D}}(q)r \le \tilde{\sigma}_3 \, \|r\|^2 \,. \tag{27}$$

$$\beta \|e\| \|e_c^{(j)}\| \le \frac{\beta^2 \epsilon^{(j)^2}}{4} \|e\|^2 + \frac{1}{\epsilon^{(j)^2}} \|e_c^{(j)}\|^2.$$
 (28)

$$||r|| \left\| Q_{1,\tau(j)}^{(j)} r_{\tau(j)} \right\| \le \frac{\varepsilon^{(j)^2}}{2} \left\| Q_{1,\tau(j)}^{(j)} r_{\tau(j)} \right\|^2 + \frac{1}{2\varepsilon^{(j)^2}} ||r||^2. \tag{29}$$

$$-\tau_i^{(j)} \int_{t-\tau_i^{(j)}}^t u_{s,i}^{(j)^2}(\theta) d\theta \le -e_{c,i}^{(j)^2}. \tag{30}$$

Remark 1. (i) In (24), σ_1 , $\sigma_2 \in \mathbb{R}_{>0}$ are minimal and maximal eigenvalues of D(q). The inequality is obtained due to the property of the inertia matrix. In (25), λ_1 , $\lambda_2 \in \mathbb{R}_{>0}$ are constants. (28) and (29) are obtained by Young's inequality and constants $\epsilon^{(j)^2}$, $\epsilon^{(j)^2}$

Z. Sheng, Z. Sun, V. Molazadeh et al. Automatica 125 (2021) 10945

 $\in \mathbb{R}_{>0}. \ (30) \ \text{is obtained by Cauchy-Schwarz inequality.} \ (ii) \ \ln \ (26), \\ \sigma_3^{(j)} = \max \left\{ \sqrt{\operatorname{eig} \left(H^{(j)^T}(t) H^{(j)}(t) \right)} \right\}, \ \text{where } \operatorname{eig} \left(H^{(j)}(t)^T H^{(j)}(t) \right) = \\ \left\{ \sigma_{3,1}^{(j)}, \sigma_{3,2}^{(j)} ... \sigma_{3,N}^{(j)} \right\} \ \text{are eigenvalues of} \ H^{(j)^T}(t) H^{(j)}(t). \ \text{The gains} \ K_{a,i}^{(j)} \\ \text{introduced in (5) provide some flexibility to manipulate} \ \sigma_3^{(j)} \\ \text{to reach desired ranges with bounded perturbations. Therefore,} \\ \left| \sigma_3^{(j)} \right| \leq \bar{\sigma}_3^{(j)} \in \mathbb{R}_{>0}. \ \text{The constant} \ \bar{\rho}_s = \max_i \left\{ \rho_{s,i} \right\}. \ \text{(iii) In} \\ \text{(27), } \tilde{D}(q) \in \mathbb{R}^{N \times N} \ \text{is the difference between the actual inertial matrix,} \ D(q), \ \text{and the estimate,} \ \hat{D}(q). \ \text{Similarly to (ii), there is a} \\ \text{constant} \ \tilde{\sigma}_3 \in \mathbb{R}_{\geq 0} \ \text{such that} \ \tilde{\sigma}_3 \geq \max \left\{ \sqrt{\operatorname{eig} \left(\tilde{D}^T \tilde{D} \right)} \right\}. \ \text{Similarly} \\ \text{to (25), there are eigenvalues,} \ \hat{\sigma}_1, \ \hat{\sigma}_2 \in \mathbb{R}_{>0}, \ \text{of} \ \tilde{D}(q) \ \text{such that} \\ \hat{\sigma}_1 \| r \|^2 \leq r^T \hat{D}r \leq \hat{\sigma}_2 \| r \|^2. \\ \end{cases}$

The following theorems in this section first ensure the stability of each individual subsystems based on the closed loop error dynamics derived in (17) and (21), respectively. The stability of the overall switched system is then analyzed in the next section.

A Lyapunov functional candidate is chosen as

$$V = \frac{1}{2}e^{T}e + \frac{1}{2}r^{T}Dr + \frac{1+\xi}{2}\sum_{i,j} \left(P_{1,i}^{(j)} + P_{2,i}^{(j)}\right),\tag{31}$$

where

$$P_{1,i}^{(j)} = \omega_i^{(j)} \int_{t-\tau^{(j)}}^t \left(\int_{\psi}^t u_{s,i}^{(j)^2}(\theta) d\theta \right) d\psi, \tag{32}$$

$$P_{2,i}^{(j)} = \frac{\bar{\sigma}_{3}^{(j)} \bar{\rho}_{s} \beta K_{u} \varepsilon^{(j)^{2}}}{2} \cdot \int_{t-\tau^{(j)}}^{t} \left(\frac{1+(-1)^{j+1} \operatorname{sgn}\left(r_{i}(\theta)\right)}{2} r_{i}(\theta)\right)^{2} d\theta,$$
(33)

and $\omega_i^{(j)} \in \mathbb{R}_{>0}$, $i=1,2,\ldots,N, j=1,2$. It is noted that V in (31), fuses two different Lyapunov functionals, which are used to analyze the two individual subsystems. Due to the form of r in (11) and the existence of $P_{1,i}^{(j)}$ and $P_{2,i}^{(j)}$, V is continuously differentiable within each subsystem but is discontinuous at switches.

Theorem 1 (Stability of the Subsystem When $\xi = 1$). For the closed loop error dynamics in (17), provided $\hat{\sigma}_1, \lambda_1, \lambda_2, \bar{\sigma}_3, \bar{\rho}_s, \epsilon^{(j)^2}, \epsilon^{(j)^2}$ are chosen as per Remark 1, if there exist $\omega_i^{(j)} \in \mathbb{R}_{>0}$, $i = 1, 2, \ldots, N$, $j = 1, 2, \bar{\omega}_{\tau} = \max_{i,j} \left\{ \omega_i^{(j)} \tau_i^{(j)} \right\}$, $\bar{\sigma}_{\varepsilon^2} = \max_j \left\{ \bar{\sigma}_3^{(j)} \varepsilon^{(j)^2} \right\}$ such that control gains, α , β , Q_2 , Q_4 and K_u satisfy

$$\alpha - \frac{\beta^2 \left(\epsilon^{(1)^2} + \epsilon^{(2)^2}\right)}{4} > 0, \tag{34}$$

 $\hat{D}\beta Q_2 + K_M Q_4 = \hat{\sigma}_1 \beta K_\rho I,$

$$\left(\hat{\sigma}_{1}K_{\rho} - \tilde{\sigma}_{3}\bar{\rho}_{s} - \frac{\bar{\rho}_{s}}{2}\left(\sum_{j}\frac{\bar{\sigma}_{3}^{(j)}}{\varepsilon^{(j)^{2}}} + \bar{\sigma}_{\varepsilon^{2}}\right)\right)\beta K_{u}$$

$$-\bar{\omega}_{\tau}\bar{\rho}_{s}^{2}K_{u}^{2} - K_{1} - K_{2} > 0,$$
(35)

where constants, K_{ρ} , K_1 , $K_2 \in \mathbb{R}_{>0}$, and the initial states $(e_0^T, r_0^T)^T$, are inside a region of attraction,

$$\Omega_0 = \left\{ (e^T, r^T)^T : e, r \in \mathbb{R}^N, \left\| (e^T, r^T)^T \right\| \le \sqrt{\frac{\Pi}{\lambda_2}} \right\}, \tag{36}$$

where

$$\Pi = \begin{cases} 0, & \Pi_p \le 0 \\ \Pi_p, & \Pi_p > 0 \end{cases}$$
(37)

$$\Pi_{p} = \lambda_{1} \min_{i,j} \left\{ 1, \frac{\bar{\sigma}_{3}^{(j)} \bar{\rho}_{s} \beta \varepsilon^{(j)^{2}}}{2 \lambda_{1} \tau_{i} \rho_{s,i}^{2} K_{u}} \right\} \delta \Phi^{-2} \left(2 \sqrt{K_{1} \chi} \right) \\
- \sum_{i,j} \left(P_{1,i}^{(j)} + P_{2,i}^{(j)} \right) - \delta_{1}, \tag{38}$$

then from an initial value, $V_0 \ge \Theta$, the L-K functional (31) converges semi-globally according to

$$V(t) \le V_0 \exp\left(-\varrho t\right) + \Theta\left(1 - \exp\left(-\varrho t\right)\right). \tag{39}$$

 $\delta_1 \in \mathbb{R}_{>0}$ is an arbitrarily small constant. $\chi, \varrho, \Theta \in \mathbb{R}_{>0}$ are constants derived in the proof.

The proof is provided in Appendix. It should be noted that the constants or variables to be determined in Theorem 1 can be categorized into two groups including control gains that directly affect the control inputs, and auxiliary constants for proving the stability. The former includes: the feedback gains, α and K_u , the gain, β , to modulate the delay compensation term, the diagonal gain matrix, Q_2 , to allocate the contribution ratio among the soft actuators, the constant, K_ρ , to determine the equation for online solving the matrix, Q_4 , which modulates torque contributions from motors. The latter includes the constants, $\hat{\sigma}_1$, λ_1 , λ_2 , $\bar{\sigma}_3$, $\bar{\rho}_s$, $\epsilon^{(j)^2}$, $\epsilon^{(j)^2}$, defined as per Remark 1, and K_1 , K_2 , χ , to be determined in the proof to estimate the region of attraction and the ultimate bound.

Theorem 2 (Stability of the Subsystem When $\xi = -1$). For the closed loop error dynamics in (21) and a control law in (20), the Lyapunov functional, (31), converges semi-globally from any initial value, $V'_0 \geq \Theta'$, according to

$$V \le V_0' \exp\left(-\varrho' t\right) + \Theta' \left(1 - \exp\left(-\varrho' t\right)\right),\tag{40}$$

until a uniformly ultimate bound, Θ' , is reached, provided the states $(e^T, r^T)^T$ are initially inside the region of attraction,

$$\Omega_0' = \left\{ (e^T, r^T)^T : e, r \in \mathbb{R}^N, \, \left\| (e^T, r^T)^T \right\| \le \sqrt{\frac{\Pi'}{\lambda_2}} \right\},\tag{41}$$

where

$$\Pi' = \lambda_1 \delta \Phi'^{-2} \left(\sqrt{\frac{\lambda_4}{K_{\nu,1} r_c}} \right) - \delta_1', \tag{42}$$

where the constant, $\lambda_4 = \min \{\alpha, K_v\}$, and an arbitrarily small constant, $\delta_1' \in \mathbb{R}_{>0}$. $K_{v,1} \in \mathbb{R}_{>0}$ is a constant that affects the conservative estimates of the ultimate bound and the region of attraction. $\varrho', \Theta' \in \mathbb{R}_{>0}$ are constants derived from the subsequent stability analysis.

The proof is provided in Appendix.

5. Stability of the switched system

Provided the control inputs, $u_s^{(j)}$, u_{m_l} , $u_{m_{ll}}$, are designed according to Theorems 1 and 2, then the Lyapunov functional of each subsystem is shown to converge according to either (39) or (40). The stability within each subsystem therefore refers to the bounded trajectory tracking errors. However, when switch occurs, the error state, r, and the Lyapunov functional, V, have a discontinuous jump when $\xi \in \{-1,1\}$ changes its sign. In addition, error states may locate outside the region of attraction of the individual controllers due to disturbance or initial conditions. In these situations, in order to ensure the stability of the overall switched system, $\mathcal{D}_{er\xi}$ and $\mathcal{D}'_{er\xi}$ in the switch criteria, (23), need

to be further designed as

time

$$\mathcal{D}_{er\xi} = \left\{ (e^T, r^T, \hat{\mu}^{(1)^T}, \hat{\mu}^{(2)^T}, \xi)^T \in \mathcal{U} : \\ \xi = 1, (e^T, r^T)^T \in \Omega_0^* \right\}, \tag{43}$$

$$\mathcal{D}'_{er\xi_{l}} = \left\{ (e^{T}, r^{T}, \xi)^{T} \in \mathbb{R}^{2N} \times \{-1, 1\} : \\ (e^{T}, r^{T})^{T} \in \Omega_{0}, (e^{T}, r^{T}, \xi)^{T} \in \Omega_{1_{l}} \right\}.$$

$$(44)$$

 $\mathcal{D}_{er\xi}$ is designed so that control mode II can be activated when the error states are out of the region of attraction of control mode I even when no muscle is fatigued. The set Ω_0^* is designed as $\Omega_0^* = \left\{ (e^T, r^T)^T : e, r \in \mathbb{R}^N, \left\| (e^T, r^T)^T \right\| \geq \sqrt{\frac{\Pi + \delta_1^*}{\lambda_2}} \right\}$, where $\delta_1^* \in \mathbb{R}_{>0}$ is a constant such that $\delta_1^* < \delta_1$. The purpose of adding δ_1^* is that, combined with the fact in (23) that $\mu < \overline{\mu}$, such a design avoids the Zeno behavior. The subscript $l, l \in \mathbb{Z}_{>0}$, in (44) is used to describe a piecewise continuous behavior. The following stability analysis imposes a non-empty set, Ω_1 , in (44) and shows

that the tracking errors re guaranteed to be bounded in finite

Firstly, for convenient notations in the subsequent stability analysis, we would like to describe the piecewise continuity of the switched system and how the time-dependent variables are evaluated at switch instant in the following way. The previously defined subscript, l, denotes the lth piece between the (l-1)th and lth switch. (The 0th switch refers to t = 0.) In addition, we use the subscript, "o" and "x" to represent the start and end point, respectively, of the current piece. As a result, $t_{x,l}$ denotes the time instant when the *l*th switch occurs. e_l , r_l , ξ_l and V_l represent the continuous time-dependent variables that are evaluated at the time $t_l \in [t_{x,l-1}, t_{x,l}]$. For example, $e_l = e_l(t_l)$. Next, we define the values of the state variable, e_1 , at the time instants: right after the previous switch and right before the next switch, as $e_{o,l}$ and $e_{x,l}$, respectively, i.e., $e_{o,l} = e_l(t_{x,l-1}, \xi_l^+(t_{x,l-1})), e_{x,l} = e_l(t_{x,l}, \xi_l^-(t_{x,l})).$ Similarly, we also define $r_{o,l}$, $V_{o,l}$, and $r_{x,l}$, $V_{x,l}$. We also define \hat{V}_l and $\hat{V}_{x,l-1}$, respectively, as estimates of V_l and $V_{x,l-1}$, respectively, by approximating the inertial matrix, D, in (31), by \hat{D} with an estimation error, \tilde{D} , that is defined in Remark 1 As a result, for 1 > 2,

$$V_l = \hat{V}_l + \frac{1}{2} r_l^T \tilde{D} r_l, \tag{45}$$

$$V_{x,l-1} = \hat{V}_{x,l-1} + \frac{1}{2} r_{x,l-1}^T \tilde{D} r_{x,l-1}. \tag{46}$$

Secondly, based on the estimated Lyapunov functional, we design the set Ω_{1_l} as

$$\Omega_{1_{l}} = \left\{ (e_{l}^{T}, r_{l}^{T}, \xi_{l})^{T} : e_{l}, r_{l} \in \mathbb{R}^{N}, \xi_{l} = -1, l \geq 2, \\
\frac{1}{2} e_{l}^{T} e_{l} + \frac{1}{2} r_{l}^{T} \hat{D} r_{l} + \frac{1}{2} \tilde{\sigma}_{3} \| r_{l} \|^{2} + \frac{1}{2} \tilde{\sigma}_{3} \| r_{x, l-1} \|^{2} \\
\leq \max \left\{ \Omega_{l} + \frac{1}{2} \tilde{\sigma}_{3} \| r_{x, l-1} \|^{2}, \hat{V}_{x, l-1} - \sum_{i, i} P_{2, i}^{(i)} \Big|_{t_{l}} \right\} \right\},$$
(47)

where Ω_l is given by (53) in Appendix. The following lemma shows the property of the Ω_{1_l} that will be further used in the subsequent stability analysis.

Lemma 1. $y=(e^T,r^T,\hat{\mu}^{(1)^T},\hat{\mu}^{(2)^T},\xi)^T$ is well defined on \mathcal{U} and the control inputs, $u_s^{(j)}$, (j=1,2), u_{m_l} , $u_{m_{ll}}$, are designed as in Theorems 1 and 2. For the time period between two consecutive switches, l-1 and l, $l\geq 2$, if the states, $(e_l^T,r_l^T,\xi_l)^T$ belong to the set, Ω_{1_l} , then the L-K functional V_l satisfies $V_l\leq \max\left\{\Omega_l,V_{x,l-1}-\sum_{i,j}P_{2,i}^{(j)}\Big|_{t_l}\right\}$. The set, Ω_{1_l} , is non-empty if the assumption, $\frac{\Omega_l}{\lambda_2+\tilde{\sigma}_3}>\frac{\tilde{\sigma}_3H}{\tilde{\sigma}_3}$ holds.

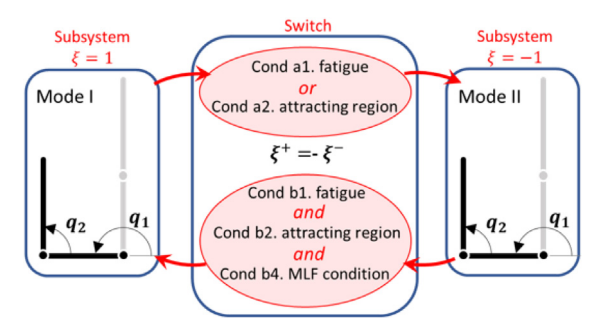


Fig. 1. A 2-link planar mechanism under the switched control.

The proof is provided in Appendix. Finally, the following theorem, which is one of the main results of this paper, guarantees the stability of the overall switched system when tracking a desired trajectory.

Theorem 3. If $y = (e^T, r^T, \hat{\mu}^{(1)^T}, \hat{\mu}^{(2)^T}, \xi)^T$ is well defined on \mathcal{U} and the followings are satisfied:

- (1) the switch criteria, \mathcal{D} , is designed according to (23), (43) and (44);
- (2) the control inputs, $u_s^{(j)}$, (j = 1, 2), u_{m_l} , $u_{m_{ll}}$, are designed as in Theorems 1 and 2;
- (3) according to Remark 2 (see Appendix), α , K_v , is chosen such that $\frac{\Omega_{II}}{\lambda_1} \leq \frac{\Omega_I}{\lambda_2 + \tilde{\sigma}_3} \frac{\tilde{\sigma}_3 \Pi}{\lambda_2 (\lambda_2 + \tilde{\sigma}_3)}$ (Ω_{II} is given by (57) in Appendix. Assume $\frac{\Omega_I}{\lambda_2 + \tilde{\sigma}_3} > \frac{\tilde{\sigma}_3 \Pi}{\lambda_2 (\lambda_2 + \tilde{\sigma}_3)}$.),

then the set, Ω_{1_l} , in (44), can be designed according to (47), such that the error states within the region of attraction can be bounded as, $\|(e^T, r^T)^T\| \le \Omega_{er}$ in finite time, where the constant, $\Omega_{er} \in \mathbb{R}_{>0}$, is given by the subsequent analysis.

The proof is provided in Appendix.

6. Simulations

To demonstrate gain selections of the designed controller, simulations are performed on trajectory tracking of a 2-link planar mechanism under the switched scheme, as illustrated in Fig. 1. Desired trajectories are generated by periodically repeated 5th order polynomials that satisfy the conditions: $q_1(2kT_{period}) = \pi$, $q_2(2kT_{period}) = \pi/2, q_1((2k+1)T_{period}) = \pi/2, q_2((2k+1)T_{period}) =$ π , $T_{period} = 10$ seconds, k = 0, 1, 2, ... First and second derivatives of q_1 , q_2 at kT_{period} are all zero. Electric motors are assigned at both joint 1 and 2 while an agonist-antagonist pair of soft actuators is assigned at joint 1. The soft actuators and their time-variant actuator efficiency are modeled according to human muscle biomechanics with a fatigue/recovery effect as in Alibeji et al. (2017) and Kirsch, Bao, Alibeji, Dicianno, and Sharma (2018). The EMDs of the two muscle groups that actuate joint 1 are set as $\tau_1^{(1)}=0.1$ sec and $\tau_1^{(2)}=0.09$ sec. Torque constant of electric motors are $K_M = \text{diag}(5.4, 5.4)$. For the subsystem of $\xi = 1$, the design and analysis of control mode I involves selections of the following constant parameters (i, j = 1, 2) that can be categorized into 2 groups:

(i) Gains that directly affect the control inputs: $\alpha=10$, $\beta=2$, $K_u=7.9$, $K_{\rho}=18$, $K_{a,i}^{(j)}=1$ (no additional modulation), $\rho_{s,1}=0.6$, $\rho_{s,2}=0$ (no soft actuator assigned at joint 2), $Q_4=\left(\rho_{m,ij}\right)_{2\times 2}$ obtained by online solving the linear algebraic

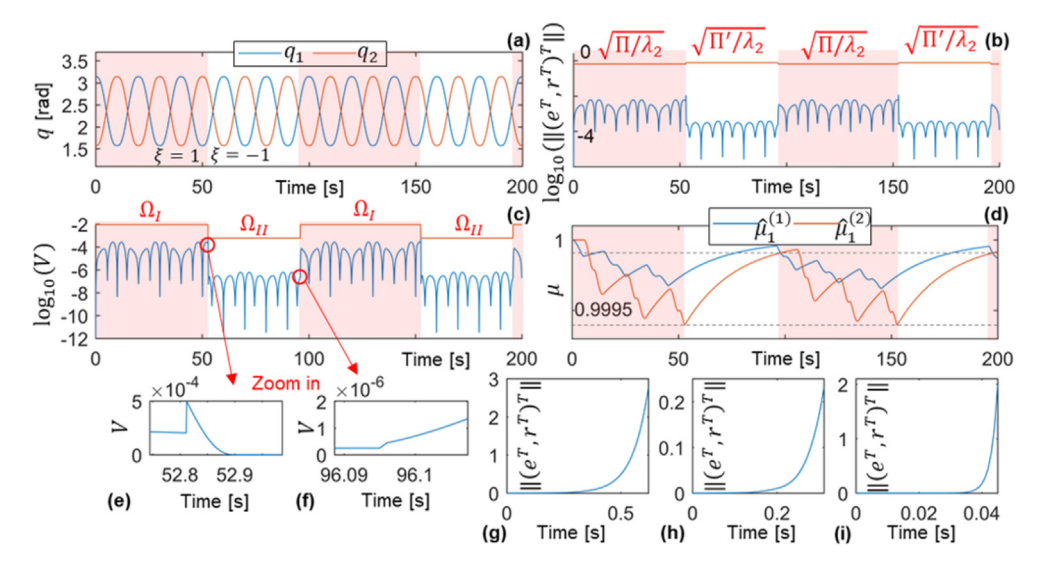


Fig. 2. Simulation result of trajectory tracking of a 2-link planar mechanism under the switched control. (a) Joint angles. (b) Norm of the error states (logarithm-scaled) and the estimated region of attraction. (c) L-K functional (logarithm-scaled) and the estimated ultimate bound. (d) Time-variant actuator efficiency, i.e., muscle fatigue and recovery. (e)–(f) Discontinuity of the L-K functional at each switch. (g)–(i) Simulated unstable situations of the subsystem, $\xi = 1$, when gain conditions are not satisfied

equation, $\hat{D}\beta Q_2 + K_M Q_4 = \hat{\sigma}_1 \beta K_\rho I$, where $\hat{\sigma}_1(t)$ is the smallest eigenvalue of the estimated inertia matrix.

(ii) Auxiliary constants selected for estimating the region of attraction and the ultimate bound: $\epsilon^{(j)} = \epsilon^{(j)} = 1$, $\omega_i^{(j)} = 4$, $\bar{\omega}_{\tau} = \max_{i,j} \left\{ \omega_i^{(j)} \tau_i^{(j)} \right\} = 0.4$, $\bar{\sigma}_3^{(1)} = 7.47$, $\bar{\sigma}_3^{(2)} = 7.41$ $\bar{\sigma}_{\varepsilon^2} = \max_j \left\{ \bar{\sigma}_3^{(j)} \epsilon^{(j)^2} \right\} = 7.47$, $\bar{\rho} = \max_i \left\{ \rho_{s,i} \right\} = 0.6$, $\tilde{\sigma}_3 = 0$ (no model uncertainty in simulations), $\lambda_1 = 0.26 \leq \min_{\forall t} \left\{ \frac{1}{2}, \frac{1}{2} \sigma_1(t) \right\}$, $\lambda_2 = 4.39 \geq \max_{\forall t} \left\{ \frac{1}{2}, \frac{1}{2} \sigma_2(t) \right\}$, $\delta \Phi (\cdot) = 10 (\cdot)$, $\Psi = 0.15$, $\chi = 8$, $K_1 = 22.80$, $K_2 = 5.00$, $\kappa_i^{(j)} = 3.10$, $\gamma_i^{(j)} = 2.47$, $\lambda_3 = 6.88 \leq \min_{i,j} \left\{ \chi - \frac{\delta \Phi^2(||z||)}{4K_1}, \frac{\lambda_2 \left(\kappa_i^{(j)} - \gamma_i^{(j)}\right)}{\tau_i^{(j)}}, \frac{2\lambda_2 \gamma_i^{(j)} \rho_{s,i}^2 K_u}{\bar{\sigma}_3^{(j)}} \bar{\rho}_{s,k}^2 K_u} \right\}$.

As a result, control gains listed in (i) satisfy all the gain conditions described in Theorem 1. A conservative estimate of the ultimate bound of V(t) when $\xi = 1$ is given by $V(t) < \frac{\lambda_2 \Psi^2}{4\lambda_3 K_2} = 0.91 \times 10^{-2}$. The region of attraction is estimated according to

Theorem 1, as
$$\|(e^T, r^T)^T\| < \sqrt{(1.90 - \sum_{i,j} \left(P_{1,i}^{(j)} + P_{2,i}^{(j)}\right))/4.39}$$
, where $P_{1,i}^{(j)}$ and $P_{2,i}^{(j)}$ are computed online. For the subsystem of $\xi = -1$, the control input is determined according to Theorem 2 with control gains $r_c = 0.001$, $K_v = 10$, and a guessing function, $\delta \Phi'(\|y_{er}\|) \|y_{er}\| + \Psi' = 10 \|y_{er}\|^2 + 1 + \|\Phi_d\|$, to bound the uncertainties. As a result, by selecting the auxiliary constants according to the proof of Theorem 2, $K_{v,1} = 10$, $K_{v,2} = 0.69$, $\Psi'' = 0.0014 \ge \frac{r_c}{4K_{v,1}} + \frac{r_c\Psi'^2}{4K_{v,2}} + K_{v,2}r_c$, $\lambda_4 = \min\{\alpha, K_v\} = 10$, $\lambda_5 = 10.00 \le \lambda_4 - K_{v,1}r_c\delta\Phi'^2$ ($\|y_{er}\|$), the ultimate bound of $V(t)$ when $\xi = -1$ is estimated by $\frac{\lambda_2\Psi''}{\lambda_5} = 0.62 \times 10^{-5}$ while the region of attraction is estimated by $\sqrt{\lambda_1\delta\Phi'^{-2}(\sqrt{\frac{\lambda_4}{K_{v,1}r_c}})/\lambda_2} = 0.77$. After obtaining the estimated region of attraction and the ultimate bound of $V(t)$ for both $\xi = 1$ and $\xi = -1$, the complete switch private as a part of complete switch private as a part of complete switch as a part of the private as a part of complete switch private as a part of complete switch as a part of the private as a part of complete switch private as a part of the private as a part of the private as a part of the private symbol designed as a part of $V(t)$ and $V($

obtaining the estimated region of attraction and the ultimate bound of V(t) for both $\xi=1$ and $\xi=-1$, the complete switch criteria can be designed according to (22), (23), (43), (44) and (47), where the thresholds for actuator efficiency are selected as $\mu=0.9994$, $\overline{\mu}=0.9999$. Fig. 2(a)–(d) summarizes the simulation results. Due to the combination of two different Lyapunov functionals as in (31), the discontinuities at switches can be observed in Fig. 2e and Fig. 2f. Fig. 2(g)–(i) list some examples when the subsystem, $\xi=1$, is unstable by violating the gain conditions.

Specifically, in Fig. 2g, β is set to 0. This eliminates the delay compensation term and makes (35) impossible to be satisfied. In Fig. 2h, $\beta=0.1$, $K_u=100$. A small β and an over amplified K_u makes (35) impossible to hold with positive constants, K_1 , K_2 . In Fig. 2i, $\alpha=1$ and $\beta=20$ makes (34) difficult to be satisfied unless $\epsilon^{(j)}$ are chosen as very small numbers. However, this will amplify $\omega_i^{(j)}$ in order to guarantee the existence of a positive χ . According to (35), large $\omega_i^{(j)}$ will further restrict the choice of K_u , K_1 and K_2 to be small numbers. As a result, according to (53) (in Appendix), the ultimate bound will be greatly amplified, although it does not go to infinity.

7. Experiments

The control design is also demonstrated in a human sittingto-standing task using a wearable 4-DOF hybrid neuroprosthetic system as shown in Fig. 3. We consider it as a combination of two 2-DOF serial human-robot system that includes the parts of the right leg and the left leg. Each part is modeled and controlled as an individual 2-DOF system, where the absolute knee angle with respect to the horizontal direction and the relative hip angle referenced to the thigh link are regarded as two independent variables. Each knee joint can be actuated by the torque produced by stimulated contractions of a quadriceps-hamstring muscle pair, as well as by an electric motor (Harmonic Drive LLC, USA). The stimulation is achieved using a commercial stimulator (Rehastim 1, HASOMED GmbH, Germany) through electrode pads (Dura-Stick Plus, 6.98 cm by 12.70 cm, Chattanooga, DJO LLC, USA). Each hip joint can be actuated by an electric motor. Joint angles are measured by internal relative encoders of the electric motors. The actuator efficiency refers to the fatigue level of human muscles under continuous stimulation and is predicted by the differential equations reported in Alibeji et al. (2017) and Kirsch et al. (2018). The controller is implemented and programmed in a real time XPC target (Speedgoat GmbH, Switzerland) using MATLAB/Simulink (MathWorks, USA). The input delay known as the EMD in each muscle was measured using the procedure as described in Alibeji et al. (2017). The results were summarized as: 90 ms for left quadriceps, 110 ms for left hamstring, 86 ms for right quadriceps, 90 ms for right hamstring.

The control objective is to track desired trajectories in repeated siting-to-standing tasks and show a automatic switch

Fig. 3. The experiment record of able-bodied human sitting-to-standings with assistance from the wearable robotic system.

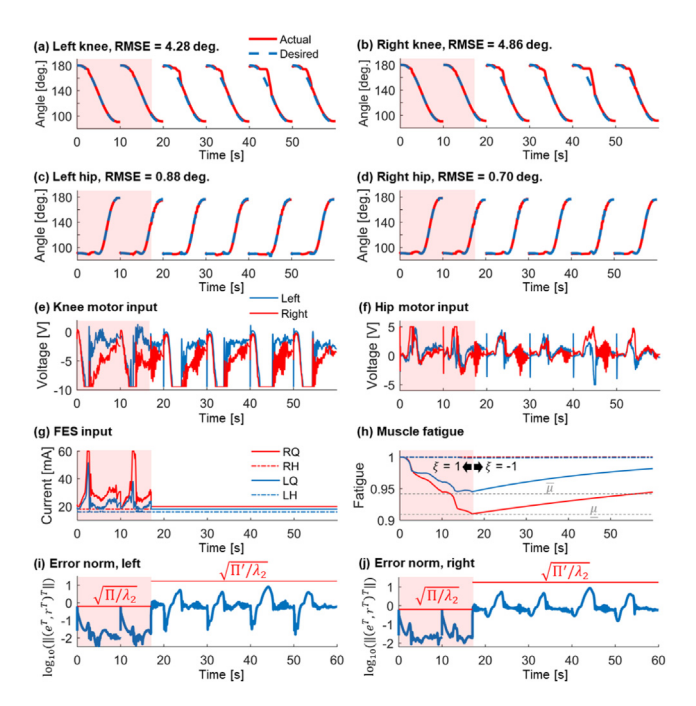


Fig. 4. Trial 1 of the sitting-to-standing experiment. (a)–(d) The desired angle trajectories and the measured joint angles. (e)–(g) Recorded control inputs from electric motors and the stimulation input current of the right (R) and left (L) quadriceps (Q) and hamstring (H) muscles. (h) Actuator efficiency curve. The lower and upper thresholds (gray dashed lines) for this trial were set as 0.91 and 0.94, respectively. (i)–(j) Norm of the tracking error in radians (logarithm-scaled, blue curve) compared to the region of attraction (red curves). (For interpretation of the references to color in this figure legend, the reader is referred to the web version of this article.)

between control mode I and II, which is determined by the complete switch criteria including the actuator efficiency, or muscle fatigue, as well as the derived stability conditions. The desired trajectories are generated from normal human sitting-to-standing profiles. The trajectories of knee angles are computed offline by polynomial fitting while the trajectories of hip angles are generated online as functions of the actual measured knee angles according to a designed virtual constraint (Molazadeh, Sheng, Bao, & Sharma, 2019) between the knee and hip joints. For both left and right part, the feedback control gains used in control mode I were: $\alpha = 20$, $\beta = 2$, $K_u = 4$, $K_\rho = 10$, $\rho_{s,1} =$ 0.5, $\rho_{s,2}=0$ (no soft actuator assigned at hip joints), $Q_4=$ $(\rho_{m,ij})_{2\times 2}$ obtained by online solving the linear algebraic equation, $\hat{D}\beta Q_2 + K_M Q_4 = \hat{\sigma}_1 \beta K_0 I$, where $\hat{\sigma}_1(t)$ is the smallest eigenvalue of the estimated inertia matrix and the motor constant matrix, $K_M = \text{diag}(5.4, 5.4)$. The feedback controller of mode II was implemented by setting $\alpha = 20$, $r_c = 0.001$, $K_v = 10$ and $\delta \Phi'(\|y_{er}\|) \|y_{er}\| + \Psi' = 10 \|y_{er}\|^2 + 15 + \|\Phi_d\|$. By selecting the auxiliary constants according to the same procedure as in the Simulations section, we can approximate the regions of attraction as, 0.63 and 17.37, for control mode I and II, respectively.

Table 1RMSE between each desired trajectory and the corresponding joint angle of the left knee (LK), right knee (RK), left hip (LH) and right hip (RH) in three individual trials.

	Number	RMSE (°)				Switch threshold	
	of standing	LK	RK	LH	RH	$\overline{\mu}$	$\underline{\mu}$
Trial 1	6	4.28	4.86	0.88	0.70	0.94	0.91
Trial 2	5	2.38	2.69	1.03	1.00	0.98	0.96
Trial 3	3	2.74	3.16	0.93	0.69	0.97	0.93

All the procedures and protocols of the experiments were approved by the Institutional Review Board (IRB) of the University of Pittsburgh. A male able-bodied human participant consented to participate in the experiments. Three trials were performed. During each trial, the participant was asked to perform a regular siting-to-standing task without knowing the desired trajectories. To demonstrate the switch behavior, in each trial, different thresholds for the efficiency state were set. In each trial, the sitting-to-standing tasks were repeated multiple times until either of the following situations occurs: (1) switches happen from control mode I to II and from II back to I. (2) 6 sitting-to-standing tasks were performed in each of the trial. The number of sittingto-standing tasks was limited to follow the approved IRB protocol. The control performance were assessed by root mean square errors summarized by Table 1. Fig. 4 is a graphic presentation of the experiment result from trial 1. The shadowed region indicates control mode I when there are stimulation inputs and muscles are fatiguing while the rest indicates control mode II when muscles are experiencing recovery. The border between the shadowed and blank region is the time instant when all the switch criteria are met and a switch occurs.

8. Conclusion

A general N-DOF switched system is formulated for a class of wearable robotic systems. The developed control framework switches between two control modes: a PD-based robust controller with designed delay compensation terms, which facilitates the distinct input delays and the unilateral actuation of the human muscle, and a smooth VSC, which is robust to disturbance and uncertainties during the recovery period of a soft actuator. An overall sGUUB stability result is achieved through an MLF approach. The stability analysis also suggests a way to impose additional constraints on the switch that were primarily driven by the state of the actuator efficiency. Simulations demonstrate the gain selections and the conservative estimate of the region of attraction, as well as the ultimate bound. Repeated human sittingto-standing experiments validate the automatic switch behavior, subject to a user-defined switch threshold of the actuator efficiency state. The reported RMSEs show a practically acceptable control error range.

Appendix

Proof of Theorem 1. When $\xi = 1$, by taking the time derivative of V in (31), substituting the closed loop error dynamics (17) into the right hand side of the differentiated (31) and applying (26), the following can be obtained.

$$\dot{V}(t) \leq -\alpha \|e\|^{2} - \left(\hat{\sigma}_{1}K_{\rho} - \tilde{\sigma}_{3}\bar{\rho}_{s}\right)\beta K_{u} \|r\|^{2}
+ \beta \|e\| \sum_{j} \|e_{c}^{(j)}\| + \|r\| \delta \Phi(\|z\|) \|z\| + \Psi \|r\|
+ \sum_{j} \beta \sigma_{3}^{(j)}\bar{\rho}_{s}K_{u} \|r\| \|Q_{1\tau(j)}^{(1)}r_{\tau(j)}\|
+ \sum_{i,j} \Gamma_{1,i}^{(j)} + \sum_{i,j} \Gamma_{2,i}^{(j)} + \sum_{i,j} \Gamma_{3,i}^{(j)},$$
(48)

where

$$\begin{split} \Gamma_{1,i}^{(j)} &= -\omega_i^{(j)} \int_{t-\tau_i^{(j)}}^t u_{s,i}^{(j)^2}(\theta) d\theta, \\ \Gamma_{2,i}^{(j)} &= \omega_i^{(j)} \tau_i^{(j)} \rho_{s,i}^2 \left(\frac{1+(-1)^{j+1} \mathrm{sgn}\left(r_i\right)}{2} \right)^2 K_u^2 r_i^2, \\ \Gamma_{3,i}^{(j)} &= \frac{\bar{\sigma}_3^{(j)} \bar{\rho}_s \beta K_u \varepsilon^{(j)^2}}{2} \left(\left(\frac{1+(-1)^{j+1} \mathrm{sgn}\left(r_i\right)}{2} r_i \right)^2 - \left(\frac{1+(-1)^{j+1} \mathrm{sgn}\left(r_{\tau_i^{(j)}}\right)}{2} r_{\tau_i^{(j)}}^2 \right)^2 \right). \end{split}$$

Using the Cauchy-Schwartz inequality in (30) and the definition of $e_{c,i}^{(j)}$ from (13), it can be derived that

$$-\omega_{i}^{(j)} \int_{t-\tau^{(j)}}^{t} u_{s,i}^{(j)^{2}}(\theta) d\theta \le -\frac{\left(\omega_{i}^{(j)} - \kappa_{i}^{(j)}\right)}{\tau^{(j)}} e_{c,i}^{(j)^{2}}, \tag{49}$$

where $\kappa_i^{(j)} \in \mathbb{R}_{>0}$, is a constant and is chosen such that $\omega_i^{(j)} - \kappa_i^{(j)} - \frac{\tau_i^{(j)}}{\epsilon^{(j)^2}} > 0$. By using (49), Young's inequalities, (28), (29), it can be further derived from (48) that

$$\dot{V}(t) \leq -\left(\alpha - \frac{\beta^{2}\left(\epsilon^{(1)^{2}} + \epsilon^{(2)^{2}}\right)}{4}\right) \|e\|^{2}
-\left(\left(\hat{\sigma}_{1}K_{\rho} - \tilde{\sigma}_{3}\bar{\rho}_{s}\right)\beta K_{u} - \sum_{j} \frac{\bar{\sigma}_{3}^{(j)}\bar{\rho}_{s}\beta K_{u}}{2\epsilon^{(j)^{2}}} \right)
- \bar{\omega}_{\tau}\bar{\rho}_{s}^{2}K_{u}^{2} - \frac{\bar{\sigma}_{\varepsilon^{2}}\bar{\rho}_{s}\beta K_{u}}{2}\right) \|r\|^{2}
- \sum_{i,j} \left(\frac{\omega_{i}^{(j)} - \kappa_{i}^{(j)}}{\tau_{i}^{(j)}} - \frac{1}{\epsilon^{(1)^{2}}}\right) e_{c,i}^{(j)^{2}}
- \sum_{i,j} \kappa_{i}^{(j)} \int_{t-\tau_{i}^{(j)}}^{t} u_{s,i}^{(j)^{2}}(\theta) d\theta
+ \|r\| \delta\Phi(\|z\|) \|z\| + \Psi \|r\|.$$
(50)

According to the designed control input in (15) and due to the fact that $\int_{t-\tau_i^{(j)}}^t \left(\int_{\psi}^t u_{s,i}^{(j)^2}(\theta)d\theta\right)d\psi \leq \tau_i^{(j)} \sup_{t-\tau_i^{(j)} \leq \psi \leq t} \int_{\psi}^t u_{s,i}^{(j)^2}(\theta)d\theta = \tau_i^{(j)} \int_{t-\tau_i^{(j)}}^t u_{s,i}^{(j)^2}(\theta)d\theta$, it can be proven that

$$-\kappa_{i}^{(j)} \int_{t-\tau_{i}^{(1)}}^{t} u_{s,i}^{(j)^{2}}(\theta) d\theta$$

$$\leq -\frac{\left(\kappa_{i}^{(j)} - \gamma_{i}^{(1)}\right)}{\tau_{i}^{(j)}\omega_{i}^{(j)}} P_{1,i}^{(j)} - \frac{2\gamma_{i}^{(j)}\rho_{s,i}^{2}K_{u}}{\bar{\sigma}_{3}^{(j)}\bar{\rho}_{s}\beta\varepsilon^{(j)^{2}}} P_{2,i}^{(j)},$$

where the constant, $\gamma_i^{(j)} \in \mathbb{R}_{>0}$, are selected such that $\gamma_i^{(j)} < \kappa_i^{(j)}$. Therefore, by defining $\chi \leq \min\{\alpha - \frac{\beta^2\left(\epsilon^{(1)^2} + \epsilon^{(2)^2}\right)}{4}, \Lambda_1, \Lambda_2\}$, where $\Lambda_1 = \left(\hat{\sigma}_1 K_\rho - \tilde{\sigma}_3 \bar{\rho}_s - \frac{\bar{\rho}_s}{2} \left(\frac{\bar{\sigma}_3^{(1)}}{\epsilon^{(1)^2}} + \frac{\bar{\sigma}_3^{(2)}}{\epsilon^{(2)^2}} + \bar{\sigma}_{\epsilon^2}\right)\right) \beta K_u - \bar{\omega}_\tau \bar{\rho}_s^2 K_u^2 - K_1 - K_2$, $\Lambda_2 = \min_{i,j} \left\{\frac{1}{\tau_{ij}^{(j)}} \left(\omega_i^{(j)} - \kappa_i^{(j)} - \frac{\tau_i^{(j)}}{\epsilon^{(j)^2}}\right)\right\}$, and by completing squares, (50) can be further bounded as

$$\begin{split} \dot{V} & \leq -\left(\chi - \frac{\delta \varPhi^2(\|z\|)}{4K_1}\right) \|z\|^2 - \left(\frac{\delta \varPhi(\|z\|) \|z\|}{2\sqrt{K_1}}\right) \\ & - \sqrt{K_1} \|r\|\right)^2 - \left(\sqrt{K_2} \|r\| - \frac{\varPsi}{2\sqrt{K_2}}\right)^2 + \frac{\varPsi^2}{4K_2} \\ & - \frac{1}{\lambda_2} \sum_j \left(\sum_i \frac{\lambda_2 \left(\kappa_i^{(j)} - \gamma_i^{(j)}\right)}{\tau_i^{(j)} \omega_i^{(j)}} P_{1,i}^{(j)} \right. \\ & - \sum_i \frac{2\lambda_2 \gamma_i^{(j)} \rho_{s,i}^2 K_u}{\bar{\sigma}_s^{(j)} \bar{\rho}_s \beta \varepsilon^{(j)^2}} P_{2,i}^{(j)}\right). \end{split}$$

Define a constant $\lambda_3 \in \mathbb{R}_{>0}$ such that $\lambda_3 \leq \min_{i,j} \left\{ \chi - \frac{\delta \Phi^2(\|z\|)}{4K_1}, \frac{\lambda_2 \left(\kappa_i^{(j)} - \gamma_i^{(j)} \right)}{\tau_i^{(j)} \omega_i^{(j)}}, \frac{2\lambda_2 \gamma_i^{(j)} \rho_{s,i}^2 K_u}{\bar{\sigma}_3^{(j)} \bar{\rho}_s \beta \varepsilon^{(j)^2}} \right\}$, where the state vector z needs to satisfy $\chi > \frac{\delta \Phi^2(\|z\|)}{4K_1}$. Due to the fact that $-\|z\| \leq -\|y_{er}\|$, \dot{V} can be further bounded as,

$$\dot{V} \leq -\lambda_3 \left(\|y_{er}\|^2 + \frac{1}{\lambda_2} \sum_{i,j} \left(P_{1,i}^{(j)} + P_{2,i}^{(j)} \right) \right) + \frac{\Psi^2}{4K_2}.$$
 (51)

Due to (25),

$$\dot{V} \le -\frac{\lambda_3}{\lambda_2}V + \frac{\Psi^2}{4K_2}.$$

By the comparison lemma (Khalil, 2002), V(t) associated with $\xi = 1$ can be solved as,

$$V(t) \le V(0) \exp\left(-\frac{\lambda_3}{\lambda_2}t\right) + \frac{\lambda_2 \Psi^2}{4\lambda_3 K_2} \left(1 - \exp\left(-\frac{\lambda_3}{\lambda_2}t\right)\right), \quad (52)$$

when the initial value, $V(0) \geq \frac{\lambda_2 \Psi^2}{4\lambda_3 K_2}$. When $V(0) < \frac{\lambda_2 \Psi^2}{4\lambda_3 K_2}$, it is obvious that V(t) will never exceed $\frac{\lambda_2 \Psi^2}{4\lambda_3 K_2}$. Therefore, for an arbitrarily small constant, $\delta_2 \in \mathbb{R}_{>0}$, a uniform ultimate bound of V can be estimated as

$$\Omega_I = \delta_2 + \frac{\lambda_2 \Psi^2}{4\lambda_2 K_2}.\tag{53}$$

By using (52) and (53), the ultimate time can be solved as, $\frac{\lambda_2}{\lambda_3} \ln \left(\frac{V(0)}{\delta_2} - \frac{\lambda_2 \Psi^2}{4\delta_2 \lambda_3 K_2} \right)$. Note that (51) holds when $\chi > \frac{\delta \Phi^2(\|z\|)}{4K_1}$. Therefore, the region of attraction, Ω_0 , can be derived by letting $\chi > \frac{\delta \Phi^2(\|z\|)}{4K_1}$ or $\|z\|^2 < \delta \Phi^{-2} \left(2 \sqrt{K_1} \chi \right)$ hold, $\forall (e^T, r^T)^T \in \Omega_0$. As a result, a conservative estimate of the region of attraction is provided as in (36).

Proof of Theorem 2. When $\xi = -1$, by taking the time derivative of V in (31), substituting the closed loop error dynamics (21) into the result, completing the squares, \dot{V} can be bounded as

$$\dot{V} \leq -\alpha \|e\|^{2} - K_{v} \|r\|^{2}
+ \frac{r_{c}\delta\Phi'(\|y_{er}\|)}{\|r\| + r_{c}} \|y_{er}\| \|r\| + \frac{r_{c}\Psi'}{\|r\| + r_{c}} \|r\| .$$

$$\leq -\left(\lambda_{4} - K_{v,1}r_{c}\delta\Phi'^{2}(\|y_{er}\|)\right) \|y_{er}\|^{2}$$
(54)

$$- \left(\frac{\sqrt{r_{c}} \|r\|}{2\sqrt{K_{v,1}} (\|r\| + r_{c})} - \sqrt{K_{v,1}r_{c}} \delta \Phi' (\|y_{er}\|) \|y_{er}\| \right)^{2} \\ - \left(\frac{\sqrt{K_{v,2}r_{c}} \|r\|}{(\|r\| + r_{c})} - \frac{\sqrt{r_{c}} \Psi'}{2\sqrt{K_{v,2}}} - \right)^{2} + \Psi'',$$

where the constants, $K_{v,1}, K_{v,2} \in \mathbb{R}_{>0}$, and $\Psi'' \ge \frac{r_c}{4K_{v,1}} + \frac{r_c\Psi'^2}{4K_{v,2}} + K_{v,2}r_c$. Define a positive constant, $\lambda_5 \le \lambda_4 - K_{v,1}r_c\delta\Phi'^2$ ($\|y_{er}\|$) and $\|y_{er}\|$ needs to satisfy

$$||y_{er}||^2 < \delta \Phi'^{-2}(\sqrt{\frac{\lambda_4}{K_{\nu,1}r_c}}).$$
 (55)

As a result, (54) becomes

$$\dot{V} \leq -\frac{\lambda_5}{\lambda_2} \left(\frac{1}{2} e^T e + \frac{1}{2} r^T D r \right) + \Psi''$$

$$\leq -\frac{\lambda_5}{\lambda_2} V + \Psi''.$$

By the comparison lemma (Khalil, 2002), V can be solved as

$$V(t) \le V_0' \exp\left(-\frac{\lambda_5}{\lambda_2}t\right) + \frac{\lambda_2 \Psi''}{\lambda_5} \left(1 - \exp\left(-\frac{\lambda_5}{\lambda_2}t\right)\right),\tag{56}$$

when the initial value, $V_0' \geq \frac{\lambda_2 \Psi''}{\lambda_5}$. When starting from an initial value, $V_0' < \frac{\lambda_2 \Psi''}{\lambda_5}$, V(t) will be always smaller than $\frac{\lambda_2 \Psi''}{\lambda_5}$. For the same δ_2 , as in (53), a uniform ultimate bound of V can be estimated as

$$\Omega_{II} = \delta_2 + \frac{\lambda_2 \Psi''}{\lambda_5}.\tag{57}$$

The ultimate time is solved as $t = \frac{\lambda_2}{\lambda_5} \ln \left(\frac{V_0'}{\delta_2} - \frac{\lambda_2 \Psi''}{\delta_2 \lambda_5} \right)$. By using (55), the region of attraction can be estimated as is given in Theorem 2.

Remark 2. Because $\lim_{r_c \to 0} \Psi'' = 0$ and $\lim_{r_c \to 0} \Pi' = \infty$, the control gains, α , K_v , r_c can always be tuned such that the region of attraction, Ω'_0 , is arbitrarily large while the ultimate bound, $\sqrt{\frac{\Omega_{II}}{\lambda_1}}$, is arbitrarily small.

Proof of Lemma 1. According to (27), it can be shown that,

$$\frac{1}{2}e_{l}^{T}e_{l} + \frac{1}{2}r_{l}^{T}\hat{D}r_{l} + \frac{1}{2}r_{l}^{T}\tilde{D}r_{l} - \frac{1}{2}r_{x,l-1}^{T}\tilde{D}r_{x,l-1}
\leq \frac{1}{2}e_{l}^{T}e_{l} + \frac{1}{2}r_{l}^{T}\hat{D}r_{l} + \frac{1}{2}\tilde{\sigma}_{3} \|r_{l}\|^{2} + \frac{1}{2}\tilde{\sigma}_{3} \|r_{x,l-1}\|^{2}.$$
(58)

Therefore, by using (45), (46), and (58), we can prove that, when $\Omega_I + \frac{1}{2}\tilde{\sigma}_3 \|r_{x,l-1}\|^2 < \hat{V}_{x,l-1} - \sum_{i,j} P_{2,i}^{(j)}\Big|_{t_l}$, satisfying the inequality in (47) indicates $V_l \leq V_{x,l-1} - \sum_{i,j} P_{2,i}^{(j)}\Big|_{t_l}$. When $\Omega_I + \frac{1}{2}\tilde{\sigma}_3 \|r_{x,l-1}\|^2 \geq \hat{V}_{x,l-1} - \sum_{i,j} P_{2,i}^{(j)}\Big|_{t_l}$, due to (27) and (45), satisfying the inequality in (47) indicates $V_l \leq \Omega_I$. Consequently, it can be obtained that

$$V_{l} \le \max \left\{ \Omega_{l}, V_{x,l-1} - \sum_{i,j} P_{2,i}^{(j)} \Big|_{t_{l}} \right\}.$$
 (59)

In order to ensure the existence of a non-empty Ω_{1_l} , a solution should exist, when $\xi_l = -1$, for the inequality in (47). A sufficient condition for this is that $\frac{1}{2}e_l^Te_l + \frac{1}{2}r_l^T\hat{D}r_l + \frac{1}{2}\tilde{\sigma}_3 \|r_l\|^2 + \frac{1}{2}\tilde{\sigma}_3 \|r_{x,l-1}\|^2 \leq \max\left\{\Omega_l - \frac{1}{2}r_{x,l-1}^T\tilde{D}r_{x,l-1}, \hat{V}_{x,l-1} - \sum_{l,j} P_{2,i}^{(j)}\Big|_{t_l}\right\}$. By adding the term, $\frac{1}{2}r_{x,l-1}^T\tilde{D}r_{x,l-1}$ to both sides, this inequality is then

equivalent to

$$V_{l} - \frac{1}{2} r_{l}^{T} \tilde{D} r_{l} + \frac{1}{2} r_{x,l-1}^{T} \tilde{D} r_{x,l-1} + \frac{1}{2} \tilde{\sigma}_{3} \| r_{l} \|^{2}$$

$$+ \frac{1}{2} \tilde{\sigma}_{3} \| r_{x,l-1} \|^{2} \leq \max \{ \Omega_{l}, V_{x,l-1} - \sum_{i,i} P_{2,i}^{(j)} \Big|_{t_{l}} \}.$$

$$(60)$$

The left hand side can be upper bounded by $V_l + \tilde{\sigma}_3 \|r_l\|^2 + \tilde{\sigma}_3 \|r_{x,l-1}\|^2$ while the right hand side can be lower bounded by Ω_l . In addition, according to (36) and due to the fact that $\xi_{l-1} = 1$, it can be derived that $\|r_{x,l-1}\|^2 \leq \frac{\Pi}{\lambda_2}$. Therefore, a non-empty solution set of (60) can be guaranteed if $V_l + \tilde{\sigma}_3 \|r_l\|^2 + \frac{\tilde{\sigma}_3 \Pi}{\lambda_2} \leq \Omega_l$ has a solution. To achieve this, by using (25), we can impose $\lambda_2 \|e_l\|^2 + (\lambda_2 + \tilde{\sigma}_3) \|r_l\|^2 \leq (\lambda_2 + \tilde{\sigma}_3) \|(e_l^T, r_l^T)^T\|^2 \leq \Omega_l - \frac{\tilde{\sigma}_3 \Pi}{\lambda_2}$ and obtain the condition

$$\|(e_l^T, r_l^T)^T\| \le \sqrt{\frac{\Omega_l}{\lambda_2 + \tilde{\sigma}_3} - \frac{\tilde{\sigma}_3 \Pi}{\lambda_2 (\lambda_2 + \tilde{\sigma}_3)}}.$$
 (61)

When $\xi=-1$ and the current subsystem is controlled by mode II, the control gains α , K_v and r_c can be tuned according to Theorem 2 and Remark 2 to obtain a small enough ultimate bound of $(e_l^T, r_l^T)^T$. Therefore, (61) can always be satisfied in finite time as long as the assumption, $\frac{\Omega_l}{\lambda_2 + \tilde{\sigma}_3} > \frac{\tilde{\sigma}_3 \Pi}{\lambda_2 (\lambda_2 + \tilde{\sigma}_3)}$, holds. This assumption is true if the estimate, D, of the inertial matrix, D, is accurate enough.

Proof of Theorem 3. Without loss of generality, we assume initially $\xi=1$ so that $\xi_l=(-1)^{l+1},\ l=1,2,3...$, when experiencing switches. By using (31), (52), (56), when all the conditions in Theorem 3 are satisfied, the following properties can be obtained.

If
$$V_{o,l} \ge S_l$$
:
$$V_l \le V_{o,l} \exp\left(-\varphi_l \left(t_l - t_{x,l-1}\right)\right) + S_l \left(1 - \exp\left(-\varphi_l \left(t_l - t_{x,l-1}\right)\right)\right),$$
If $V_{c,l} \le S_l$:
(62)

$$\begin{aligned}
&\text{If } V_{o,l} \leq S_l: \\
&V_l \leq S_l.
\end{aligned} \tag{63}$$

$$V_{x,2k} = V_{0,2k+1} - \sum_{i,j} P_{2,i}^{(j)} \Big|_{t_{x,2k}}, \ k \in \mathbb{Z}_{>0}.$$
 (64)

$$|V_{0,2k} - V_{x,2k-1}| = \Delta|_{t=t_{x,2k-1}} \in \mathcal{L}_{\infty}, \ k \in \mathbb{Z}_{>0}.$$
(65)

 $\varphi_l, S_l \in \mathbb{R}_{>0}$ are used to combine (52) and (56) in a general form and $S_{2k-1} = \frac{\lambda_2 \Psi^2}{4\lambda_3 K_2}$, $S_{2k} = \frac{\lambda_2 \Psi''}{\lambda_5}$, $k \in \mathbb{Z}_{>0}$. (64) holds because $P_{1,i}^{(j)} = e_{c,i}^{(j)} = 0$, at time $t_{x,2k}$. In (65), $\Delta = \left| \sum_{i,j} \left(P_{1,i}^{(j)} + P_{2,i}^{(j)} \right) + \frac{1}{2} (\dot{e} + \alpha e - \beta e_c)^T D(\dot{e} + \alpha e - \beta e_c) - \frac{1}{2} (\dot{e} + \alpha e)^T D(\dot{e} + \alpha e) \right|$ and $(\cdot) \in \mathcal{L}_{\infty}$ denotes boundedness. It is obvious that for any finite index l, $V_{0,l}$ and $t_{x,l} - t_{x,l-1}$ are also finite. Hence, two cases are discussed:

(i) When $l \to \infty$ as $t \to \infty$, consider the cases when l = 2k - 1 and l = 2k, $k \in \mathbb{Z}_{>0}$. When $\Omega_l < V_{x,2k-1} - \sum_{i,j} P_{2,i}^{(j)} \Big|_{t_{x,2k}}$, then due to Lemma 1, Ω_{1_l} in (47) forces $V_{x,2k} \le \max \left\{ \Omega_l, V_{x,2k-1} - \sum_{i,j} P_{2,i}^{(j)} \Big|_{t_{x,2k}} \right\}$, which implies $V_{x,2k} + \sum_{i,j} P_{2,i}^{(j)} \Big|_{t_{x,2k}} \le V_{x,2k-1}$. Further, due to (64), we have $V_{0,2k+1} \le V_{x,2k-1}$. Otherwise, when $\Omega_l > V_{x,2k-1} - \sum_{i,j} P_{2,i}^{(j)} \Big|_{t_{x,2k}}$, we have $V_{x,2k} \le \Omega_l$ and $\sum_{i,j} P_{2,i}^{(j)} \Big|_{t_{x,2k}} \le \bar{P}$, where the constant $\bar{P} = \max_{\Omega_{V,1}} \left\{ \sum_{i,j} P_{2,i}^{(j)} \right\}$, $\Omega_{V,1} = \left\{ (e^T, r^T)^T : e, r \in \mathbb{R}^N, \frac{1}{2} e^T e + \frac{1}{2} r^T D r + \sum_{i,j} \left(P_{1,j}^{(j)} + P_{2,j}^{(j)} \right) \right\}$

Z. Sheng, Z. Sun, V. Molazadeh et al. Automatica 125 (2021) 109455

 $\leq \Omega_I$ In this situation, $V_{0,2k+1} = V_{x,2k} + \sum_{i,j} P_{2,i}^{(j)}\Big|_{t_{x,2k}} \leq \Omega_I + C_{x,2k}$ \bar{P} . As a result, $V_{0,2k+1} \leq \max \{\Omega_I + \bar{P}, V_{x,2k-1}\}$. In addition, due to (62) and non-existence of Zeno behavior, a finite time duration, t_{2k-1} , makes $V_{x,2k-1}$ strictly less than $V_{0,2k-1}$ by a finite positive number, i.e., $V_{x,2k-1}$ strictly less than $V_{0,2k-1}$ by a limit positive number, i.e., $V_{x,2k-1} < V_{0,2k-1}$. Therefore $V_{0,2k+1} \le \max \left\{ \Omega_I + \bar{P}, V_{x,2k-1} \right\}$ < $\max \left\{ \Omega_I + \bar{P}, V_{0,2k-1} \right\}$. This indicates that $V_{0,2k+1}$ is strictly decreasing as k increases over switches until reaching $\Omega_I + \bar{P}$ and there must exist some finite integer k^* such that $\forall k \geq k^*$, $V_{0,2k+1} \leq \Omega_I + \bar{P}$. Besides, due to the boundedness property at odd switch indices given by (65) and the convergence property given by (62), (63), it can be obtained that $\forall k > k^*, \ V_{0,2k+2} \le \Delta|_{t=t_{x,2k+1}} + V_{x,2k+1} \le \Delta|_{t=t_{x,2k+1}} + \max \left\{ S_{2k+1}, \ V_{0,2k+1} \right\} \le \max_{\Omega_{V,2}} \{\Delta\} + \max_{\Omega_{V,2}} \{\Delta\} + \sum_{t=t_{x,2k+1}} \tilde{P}_{t}, \ \text{where } \Omega_{V,2} = \left\{ (e^T, r^T)^T : e, r \in \mathbb{R}^N, \ \frac{1}{2}e^Te + \right\}$ $\frac{1}{2}r^TDr + \sum_{i,j} \left(P_{1,i}^{(j)} + P_{2,i}^{(j)}\right) \leq \Omega_I + \bar{P}$. Therefore, by combining the analysis of both odd and even switch indices, it can be concluded that $\forall l \geq 2k^* + 1$, $V_{o,l} \leq \max_{\Omega_{V,2}} \{\Delta\} + \Omega_l + \bar{P}$. By using (62), (63), as well as the fact, $\Omega_{ll} \leq \Omega_l$, which is inferred from (3) of Theorem 3, it can be obtained that $V_l \leq \max \{V_{o,l}, S_l\} \leq$ $\max\left\{\max_{\Omega_{V,2}}\left\{\Delta\right\}+\Omega_{l}+\bar{P},\tfrac{\lambda_{2}\Psi''}{\lambda_{4}},\tfrac{\lambda_{2}\Psi^{2}}{4\lambda_{3}K_{2}}\right\}\leq\max\left\{\max_{\Omega_{V,2}}\left\{\Delta\right\}+\right.$ $\Omega_{l} + \bar{P}, \Omega_{l}, \Omega_{ll}$ $\leq \max_{\Omega_{V,2}} {\{\Delta\}} + \Omega_{l} + \bar{P}$. This means that $\forall t \geq \sum_{l=1}^{2k^*} (t_{x,l} - t_{x,l-1})$ tracking error $\|(e^T, r^T)^T\| \leq \sqrt{V/\lambda_1} \leq$

 $\sqrt{(\max_{\Omega_{V,2}} \{\Delta\} + \Omega_l + \bar{P})/\lambda_1}$ and uniform ultimate boundedness result is therefore guaranteed.

(ii) When l is finite as $t \to \infty$, the proof is trivial because

(ii) When l is finite as $t \to \infty$, the proof is trivial because there is no switch after the last one. Therefore, after the last switch, V decays continuously according to Theorem 1, so that $\|(e^T, r^T)^T\| \le \sqrt{\Omega_{II}/\lambda_1}$.

It should be noted that assuming $\xi=1$ at the beginning does not reduce generality because according to the switch criteria, the switched systems of any other initial conditions will eventually switched to the subsystem with $\xi=1$ within finite time and switches. Exactly same procedure of proof can be applied after that.

References

- Alibeji, N., Kirsch, N., Dicianno, B. E., & Sharma, N. (2017). A modified dynamic surface controller for delayed neuromuscular electrical stimulation. IEEE/ASME Transactions on Mechatronics, 22(4), 1755–1764.
- Andrikopoulos, G., Nikolakopoulos, G., & Manesis, S. (2014). Advanced nonlinear PID-based antagonistic control for pneumatic muscle actuators. *IEEE Transactions on Industrial Electronics*, 61(12), 6926–6937.
- Aroche, O. N., Meyer, P.-J., Tu, S., Packard, A., & Arcak, M. (2019). Robust control of the sit-to-stand movement for a powered lower limb orthosis. IEEE Transactions on Control Systems Technology, http://dx.doi.org/10.1109/TCST.2019.2945908), (Early Access).
- Bekiaris-Liberis, N., & Krstic, M. (2012). Compensation of time-varying input and state delays for nonlinear systems. *Journal of Dynamic Systems, Measurement and Control*, 134(1), Article 011009.
- Branicky, M. S. (1998). Multiple Lyapunov functions and other analysis tools for switched and hybrid systems. *IEEE Transactions on Automatic Control*, 43(4), 475–482.
- Caldwell, D. G., Medrano-Cerda, G. A., & Goodwin, M. (1995). Control of pneumatic muscle actuators. *IEEE Control Systems Magazine*, 15(1), 40–48.
- Cempini, M., De Rossi, S. M. M., Lenzi, T., Vitiello, N., & Carrozza, M. C. (2012). Self-alignment mechanisms for assistive wearable robots: A kinetostatic compatibility method. *IEEE Transactions on Robotics*, 29(1), 236–250.
- Choo, J., & Park, J. H. (2017). Increasing payload capacity of wearable robots using linear actuators. IEEE/ASME Transactions on Mechatronics, 22(4), 1663–1673.
- Chou, C.-P., & Hannaford, B. (1996). Measurement and modeling of mckibben pneumatic artificial muscles. *IEEE Transactions on Robotics and Automation*, 12(1), 90–102.

Daerden, F., & Lefeber, D. (2002). Pneumatic artificial muscles: actuators for robotics and automation. European Journal Mechanical and Environmental Engineering, 47(1), 11–21.

- De Looze, M. P., Bosch, T., Krause, F., Stadler, K. S., & O'Sullivan, L. W. (2016). Exoskeletons for industrial application and their potential effects on physical work load. *Ergonomics*, 59(5), 671–681.
- DeCarlo, R. A., Branicky, M. S., Pettersson, S., & Lennartson, B. (2000). Perspectives and results on the stability and stabilizability of hybrid systems. *Proceedings of the IEEE*, 88(7), 1069–1082.
- Downey, R. J., Cheng, T. H., Bellman, M. J., & Dixon, W. E. (2017). Switched tracking control of the lower limb during asynchronous neuromuscular electrical stimulation: theory and experiments. *IEEE Transactions on Cybernetics*, 47(5), 1251–1262
- Goebel, R., Sanfelice, R. G., & Teel, A. R. (2009). Hybrid dynamical systems. *IEEE Control Systems Magazine*, 29(2), 28–93.
- Harib, O., Hereid, A., Agrawal, A., Gurriet, T., Finet, S., Boeris, G., et al. (2018). Feedback control of an exoskeleton for paraplegics: Toward robustly stable, hands-free dynamic walking. *IEEE Control Systems Magazine*, 38(6), 61–87.
- Huo, W., Mohammed, S., Moreno, J. C., & Amirat, Y. (2014). Lower limb wearable robots for assistance and rehabilitation: A state of the art. *IEEE Systems Journal*, 10(3), 1068–1081.
- In, H., Kang, B. B., Sin, M., & Cho, K.-J. (2015). Exo-glove: A wearable robot for the hand with a soft tendon routing system. *IEEE Robotics & Camp; Automation Magazine*. 22(1), 97–105.
- Jamwal, P. K., Xie, S. Q., Hussain, S., & Parsons, J. G. (2012). An adaptive wearable parallel robot for the treatment of ankle injuries. *IEEE/ASME Transactions on Mechatronics*, 19(1), 64–75.
- Khalil, H. (2002). Nonlinear systems (3rd ed.). Prentice Hall.
- Kim, H., Miller, L. M., Fedulow, I., Simkins, M., Abrams, G. M., Byl, N., et al. (2012). Kinematic data analysis for post-stroke patients following bilateral versus unilateral rehabilitation with an upper limb wearable robotic system. *IEEE Transactions on Neural Systems Rehabilitation Engineering*, 21(2), 153–164.
- Kirsch, N., Alibeji, N., Dicianno, B. E., & Sharma, N. (2016). Switching control of functional electrical stimulation and motor assist for muscle fatigue compensation. In *Proceedings of American Control Conference* (pp. 4865–4870).
- Kirsch, N. A., Bao, X., Alibeji, N. A., Dicianno, B. E., & Sharma, N. (2018). Model-based dynamic control allocation in a hybrid neuroprosthesis. IEEE Transactions on Neural Systems Rehabilitation Engineering, 26(1), 224–232.
- Krstic, M. (2009). Delay compensation for nonlinear, adaptive, and PDE systems. Springer.
- Kubota, S., Nakata, Y., Eguchi, K., Kawamoto, H., Kamibayashi, K., Sakane, M., et al. (2013). Feasibility of rehabilitation training with a newly developed wearable robot for patients with limited mobility. Archives of Physical Medicine and Rehabilitation, 94(6), 1080–1087.
- Lei, J., & Khalil, H. K. (2015). Feedback linearization for nonlinear systems with time-varying input and output delays by using high-gain predictors. *IEEE Transactions on Automatic Control*, 61(8), 2262–2268.
- Lei, J., & Khalil, H. K. (2016). High-gain-predictor-based output feedback control for time-delay nonlinear systems. *Automatica*, 71, 324–333.
- Liberzon, D., & Morse, A. S. (1999). Basic problems in stability and design of switched systems. IEEE Control Systems Magazine, 19(5), 59–70.
- Lv, G., & Gregg, R. D. (2017). Underactuated potential energy shaping with contact constraints: Application to a powered knee-ankle orthosis. *IEEE Transactions on Control Systems Technology*, 26(1), 181–193.
- Mirvakili, S. M., & Hunter, I. W. (2018). Artificial muscles: Mechanisms, applications, and challenges. *Advanced Materials*, 30(6), Article 1704407.
- Molazadeh, V., Sheng, Z., Bao, X., & Sharma, N. (2019). A robust iterative learning switching controller for following virtual constraints: Application to a hybrid neuroprosthesis. *IFAC-PapersOnLine*, *51*(34), 28–33.
- Nihtilä, M. T. (1989). Adaptive control of a continuous-time system with time-varying input delay. Systems & Control Letters, 12(4), 357-364.
- Polyakov, A., Efimov, D., Perruquetti, W., & Richard, J.-P. (2013). Output stabilization of time-varying input delay systems using interval observation technique. *Automatica*, 49(11), 3402–3410.
- Pons, J. L. (2008). Wearable robots: biomechatronic exoskeletons. John Wiley & Sons.
- Pons, J. L. (2010). Rehabilitation exoskeletal robotics. *IEEE Engineering in Medicine* and Biology, 29(3), 57–63.
- Reynolds, D., Repperger, D., Phillips, C., & Bandry, G. (2003). Modeling the dynamic characteristics of pneumatic muscle. *Annals of Biomedical Engineering*, 31(3), 310–317.
- Sadegh, N., & Horowitz, R. (1990). Stability and robustness analysis of a class of adaptive controllers for robotic manipulators. *International Journal of Robotics Research*, 9(3), 74–92.
- Sharma, N., Bhasin, S., Wang, Q., & Dixon, W. E. (2011). Predictor-based control for an uncertain Euler-Lagrange system with input delay. *Automatica*, 47(11), 2332–2342
- Sharma, N., Gregory, C., & Dixon, W. E. (2011). Predictor-based compensation for electromechanical delay during neuromuscular electrical stimulation. *IEEE Transactions on Neural Systems Rehabilitation Engineering*, 19(6), 601–611.

Sharma, N., Kirsch, N. A., Alibeji, N. A., & Dixon, W. E. (2017). A non-linear control method to compensate for muscle fatigue during neuromuscular electrical stimulation. Frontiers in Robotics AI, 4, 68.

Sheng, Z., Molazadeh, V., & Sharma, N. (2018). Hybrid dynamical system model and robust control of a hybrid neuroprosthesis under fatigue based switching. In *Proceedings of American Control Conference* (pp. 1446–1451).

Tondu, B., & Lopez, P. (2000). Modeling and control of mckibben artificial muscle robot actuators. *IEEE Control Systems Magazine*, 20(2), 15–38.

Vo-Minh, T., Tjahjowidodo, T., Ramon, H., & Van Brussel, H. (2010). A new approach to modeling hysteresis in a pneumatic artificial muscle using the maxwell-slip model. *IEEE/ASME Transactions on Mechatronics*, 16(1), 177–186.
 Walsh, C. (2018). Human-in-the-loop development of soft wearable robots. *Nature Reviews Materials*, 3(6), 78.

Zinober, A. S. (1994). Variable structure and Lyapunov control, Vol. 193. Springer.



Zhiyu Sheng graduated from Shanghai Jiao Tong University in 2013 with a B.S. degree in Mechanical Engineering and Automation. He then went to Columbia University in the City of New York and obtained his M.S. degree in Mechanical Engineering in 2015. In 2020, he obtained his Ph.D. degree in Mechanical Engineering at the University of Pittsburgh. His research focus is nonlinear control systems and closed-loop hybrid exoskeletons utilizing wearable ultrasound imaging sensors. He is now an International Postdoctoral Associate in the School of Medicine, Department

of Medicine, Division of Cardiology at the University of Pittsburgh.



Ziyue Sun received his B.S. and M.S. in Mechanical Engineering from the University of Pittsburgh. He is currently pursuing a Ph.D. in the Joint Department of Biomedical Engineering UNC/NCSU under the advisement of Dr. Nitin Sharma.

zsun32@ncsu.edu



Vahidreza Molzadeh received his B.S. in Aerospace Engineering from K. N. Toosi University in 2013, and then received his M.S. in Aerospace Engineering from Sharif University of Technology in 2015. He was a Ph.D. Student in Mechanical Engineering under the supervision of Dr. Sharma at University of Pittsburgh from 2016 to 2020.



Nitin Sharma received the B.E. degree in Industrial Engineering from Thapar Institute of Engineering and Technology, India, in 2004, and the M.S. degree and the Ph.D. degree in Mechanical Engineering from the Department of Mechanical and Aerospace Engineering, University of Florida, Gainesville, in 2008 and 2010 respectively. He was an Alberta Innovates-Health Solutions Post-Doctoral Fellow with the Department of Physiology, University of Alberta, Edmonton, Canada. From 2012–2017, he was an Assistant Professor with the Department of Mechanical Engineering and Mate-

rials Science, University of Pittsburgh and promoted to an Associate Professor in 2018. In 2019, he joined the Joint Department of Biomedical Engineering at North Carolina State University-Raleigh and University of North Carolina-Chapel Hill.

Research Interests: His research interests include the modeling, optimization, and control of functional electrical stimulation (FES), hybrid exoskeletons that combine FES and a powered exoskeleton. His research group has recently started looking into using ultrasound imaging derived sensing signals to address human robot interaction problems in rehabilitation. He has won O. Hugo Schuck Award for the Best Application Paper from the 2008 American Control Conference. His research in hybrid exoskeletons is funded by three NSF awards and one NIH R03 Award. He won NSF CAREER Award in 2018.